JOURNAL OF MATERIALS SCIENCE 6 (1971) 453–478

# Identification of Structural Processes in Deformation of Oriented Polyethylene

A. KELLER, D. P. POPE
*H. H. Wills Physics Laboratory, University of Bristol, Bristol BS8 1TL, UK*

The investigation is concerned with the relation between changes in the submicroscopic structure, as revealed by low angle X-ray scattering in combination with the usual wide angle X-ray diffraction, and changes in the macroscopic sample dimensions during the deformation of oriented low density polyethylene. The samples examined are mainly drawn and rolled sheets possessing a double crystal texture, with a limited additional study on a drawn sample with fibre symmetry and on recently discovered single texture specimens. The deformations include tension and compression along selected sample directions applied mostly at room temperature, but also at various elevated temperatures. The salient feature of most of these experiments is the identity of the macroscopic strain and the changes in the submicroscopic periodicity along the direction in which the sample has been initially oriented. Even when this identity is not obeyed, as for deformation at the highest temperatures, a proportionality between the quantities concerned is always maintained.

It is demonstrated how the changes in the structural periodicity can be subdivided into a rotation of unaltered crystallites, interpreted as interlamellar slip, into a change in chain inclination within the crystallites, interpreted as intralamellar slip, and into a change in the separation of the crystallites which includes the extension or compression of interlamellar amorphous material. It is shown that the relative contributions of each of these three effects is a function of the temperature of the deformation, the sample type and the type of stress applied. The results are evaluated and discussed in terms of existing conceptions of an oriented polymer and are related to earlier findings on this subject. It is pointed out in particular that the samples in question represent a very simple mechanical system: a series coupling of the individual structural processes involved suffices to describe the response of the sample to externally imposed stress.

The identity relation between changes in structure and macroscopic sample dimensions is also revealed by swelling experiments. This, in addition to equating changes in lamellar separation with changes in sample dimension, also provides some definitive information on the location of the swelling agent.

## 1. Introduction: Background and Scope of the Work

A crystalline polymer contains structures in a range of dimensional levels. On deformation all levels can be affected. Consequently, in general, the deformation of a polymer cannot be described in terms of a single structural process. When dealing with structural aspects of deformation or with its consequences for mechanical properties, the particular structures which are most affected, or which are most relevant for the purposes in question need specifying, e.g. whether we are concerned with deformation of spherulites, with rotation of lamellae, deformation of the crystal lattice, unfolding of chains originally in the crystal or straightening of random chain configurations within the amorphous component etc. Under specific circumstances one or a few of the totality of such structure changes can be more prominent than others. This will depend on the sample type in question and, for a given sample, on the temper-

ature and on the time scale of the experiment, and of course on the magnitude of the strain. Another distinction is whether the deformation is plastic or elastic. This, however, is not as useful here as in the case of simple substances because the boundary between what is plastic and elastic is not sharp and depends on the time scale in any case. Also, in structural terms we have an intricate composite where for a given macroscopic sample deformation some components may deform in a plastic manner while others are still within the elastic range of deformation.

In a series of earlier studies, we, and other investigators [1-10], have adopted the following approach. Samples were prepared so as to possess as simple a texture as possible in order that certain individual structural processes could be first identified, then studied in some detail, and subsequently correlated with mechanical behaviour [9, 10]. As a further objective it was hoped to apply the knowledge gained on such simple samples to systems with more complex textures, where the processes originally recognised in isolation may occur in combination. The work to be reported here is a continuation of this line of research. The structural units we shall be concerned with are the crystal lamellae, in particular their orientation, changes in their internal structure and in mutual separation. In order to define the purpose of the new work the rather extensive background needs to be summarised first.

The material of the past studies was low density polyethylene. It is apparent, in retrospect, that this is a very suitable material for the purpose as it is sufficiently crystalline to possess the characteristic lamellar morphology to be diagnosed by low angle X-ray diffraction and at the same time possesses sufficient amorphous material to display those characteristic properties by which polymers are distinct from other polycrystalline materials. It is the interrelation and interaction between crystals and the amorphous components on which much of the experimental material in this line of study rests. The samples were in the form of drawn films which were subsequently rolled along the draw direction. The rolling and subsequent light heat annealing led to a double texture which formed the starting point of that part of the work which is our present concern.

Adopting the previously used notation [1, 4] we define the macroscopic film by directions x, y, z as shown in fig. 1. Light heat annealing

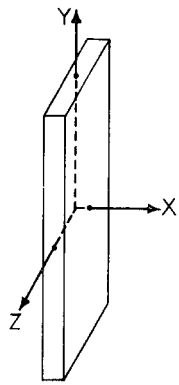


*Figure 1* The external shape of the double oriented samples used throughout the work to serve as reference throughout the paper. y = draw and roll direction, x = normal to rolling plane.

preserved the chain direction (the crystallographic *c*-axis) along the original draw direction, y, but aligned the *a*-axis along x and the *b*-axis along z (for unit cell of polyethylene see Bunn [11] or [1] and [4]). Hence we have a single crystal type texture where the three principle crystal axes are along readily identifiable directions in the macroscopic sample [4]. It is already established that a crystalline polymer consists of uniformly thick lamellae with the chains normal, or at a specified large angle, to the lamellar interface. The chains are to a large extent folded and thus confined to within a given lamella. A certain amount of chain traversing between different lamellae, however, is also part of the picture. The proportion of folding and traversing chain is a major issue in itself and the details will not concern us here (in fact even the issue of chain folding will not feature explicitly in the work except to the extent that it accounts for the individuality of the lamellae). The schematic structure of a lamella as far as it concerns the present work is shown in fig. 2. Together with the caption it contains the definition of all the quantities required for its characterisation for the present purpose.

As is well known the lamellar structure gives rise to discrete X-ray reflections at low angles by which both lamellar periodicity (i.e. thickness) and orientation can be assessed, in the simplest approximation by Bragg's law. In the simple crystal type texture referred to, the lamellar planes are parallel to z and therefore to the *b* crystal axis. Thus the lamellar normals ($n_L$) are in the xy plane [1, 2, 5]. Accordingly the lamellar

interfaces are of the $\{h0l\}$ type in terms of the polyethylene crystal structure. In the particular case in question they are $\{3\,0\,1\}$, which implies that the chains are inclined at 45° to the basal planes [5]. The lamellae are present in two distinct orientations [5] (such as shown by fig. 3a), with the morphological relation between the

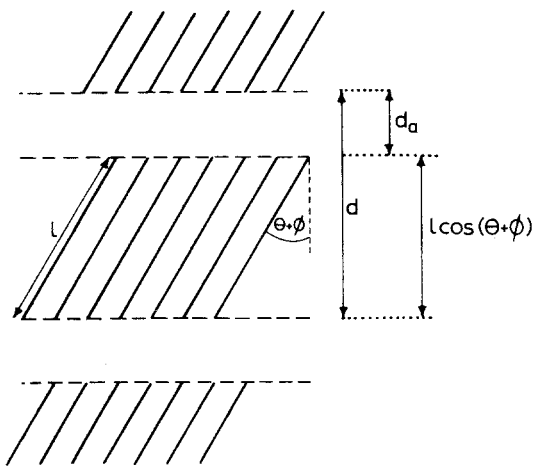


*Figure 2* Schematic representation of a lamellar sequence with the definitions of the quantities used in the paper. d is the periodicity given by the low angle X-ray spacing. It is constituted by a crystalline region $l\cos(\theta+\phi)$ and a region of different electron density of thickness $d_a$. $d_a$ contains the surface region of the lamella believed to be largely amorphous, plus whatever discontinuity there may arise in the course of lamellar packing (the two are not distinguished in the present definition of $d_a$). $l$ is the average length of the chains traversing the crystal region and $(\theta+\phi)$ their inclination. $\theta$ and $\phi$ are the two individual quantities which are measured experimentally and are defined in fig. 3.

two sets remaining unspecified from the X-ray evidence alone. Thus the starting samples in question possess a single texture as regards the unit cell ($a$, $b$, $c$) but a double texture as regards the lamellae ($n_L$).

On heating beyond the temperature at which the starting texture has been obtained ($\sim 80°C$), the sample shrinks. In the course of it both unit cell and lamellar structure undergo reorientation [5]. The chains progressively tilt away from y, and the lamellar normals $n_L$ tilt towards y while the $b$-axis remains parallel to z. This reorientation corresponds to a rotation of otherwise unaltered lamellae (fig. 3b, c) until $n_L$ becomes parallel to y (fig. 3c). Close to this stage there is also a rearrangement of the lamellar structure from a $\{301\}$ to $\{201\}$ lamellar interface which implies a change towards a lower chain obliquity [5]). We interpreted this lamellar rotation as the result of interlamellar slip activated by the internal compressive forces which are released by the heat treatment and which are responsible for the sample shrinkage [5].

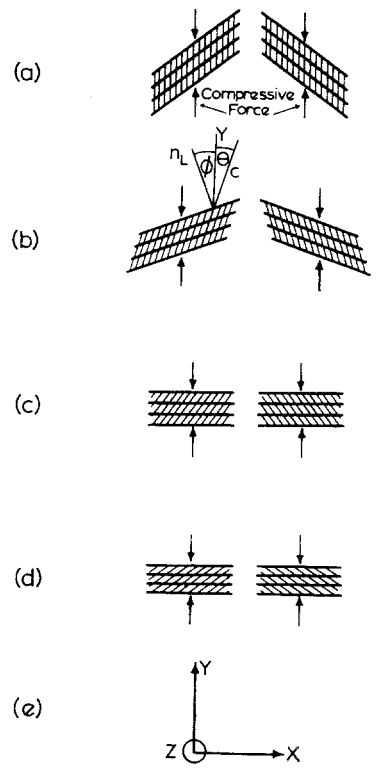


*Figure 3* Schematic illustration of the textures referred to in the text. It represents the view of the sample in fig. 1 along z. The lamellae are seen edgewise. The heavy lines represent the lamellar boundaries, the fine striations the chains (*c*-axes). The actual lamellar repeat is to be envisaged as in fig. 2.

On heating to still higher temperatures the lamellae stayed in the orientation of fig. 3c but the chains continued to tilt further away from y (fig. 3d). Evidently at this stage the lamellae themselves deform. We interpreted this phenomenon as intralamellar slip activated by the same compressive forces which have been invoked to account for the interlamellar slip above. As usual in chain folded systems the lamellar thickness also increases on these heat treatments, but this does not seem to interfere with the orientation sequence of fig. 3a-d.

In experiments which followed, the same

orientation effects, which in the above cases resulted from internal forces released by heat treatment, were produced by externally imposed stresses under isothermal conditions [5, 6, 8]. Thus, suitable samples were prepared in one of the states fig. 3a-d and were deformed at the temperature at which the particular starting state was achieved by the preceding heat treatment. When a sample as in fig. 3b was stretched along y, or compressed along x the orientation sequence fig. 3b → a was achieved [6], while samples such as in fig. 3a when compressed along y went through the orientation sequence fig. 3a → c. In neither case was there a change in lamellar thickness, only in the orientation of otherwise unaltered lamellae. When samples in the state of fig. 3c were compressed externally along y at the elevated temperature at which this sample type was originally obtained, the sequence fig. 3c → d was achieved with appropriate reduction of layer thickness [8]. Thus the previously postulated inter-and intralamellar slip processes could now be achieved by externally imposed forces, which shows that these processes are also likely to occur on externally induced deformation under more general circumstances. All these deformation experiments have, amongst others, one feature in common: changes in the sample dimensions were about 3x larger than expected from the lamellar rotation during the sequences fig. 3a ⇌ c [6] or lamellar deformation in the sequence fig. 3c → d [8]. In spite of this numerical discrepancy there was, nevertheless, a simple and reproducible relation between changes in the lamellar rotation or lamellar thickness and those in the sample dimensions, indicating a well defined underlying structure process (see [6, 8, 12]).

There is one further feature common to all these results: the deformation processes, as far as can be diagnosed by X-rays, involve only the rotation of lamellae with no change in lamellar periodicity, or where the lamellar period changes, as in the sequence fig. 3c-d, this is merely the consequence of a change in molecular inclination within the crystal. In no case is there any indication of the separation of the crystal cores being affected, i.e. of a change in $d_a$ in fig. 2. On the other hand there is a body of evidence in the literature that the long period itself increases on stretching [13, 14], in some instances accounting quantitatively for the change in sample dimension [14]. Based on these observations these workers claim that the extension of the sample results in the stretching of the amorphous material situated between the crystalline lamellae which produces the increase in long spacing. As these authors only consider the layer line periodicity and not the Bragg spacing (maxima along the layer line, when present) they would not take rotation into account if it occurred. For this reason the above results were not considered as necessarily conflicting with the picture which we have evolved, particularly as they were obtained on samples with fibre symmetry which are morphologically less well defined (see [5]). However a more recent publication by Ishikawa *et al* [15] which reports effects as in [13] and [14], both in extension and compression, leaves no doubt that there is a genuine conflict between our respective observations and conclusions. This we set out to resolve in the present work.

On reconsidering the experimental conditions adopted in the conflicting works the following differences are noted. The deformation experiments which have led to the picture of inter- and intralamellar slip were carried out on the specially prepared double texture samples and at the elevated temperatures required for obtaining the particular starting states (the photographs themselves could be taken at these temperatures or after cooling to room temperature, the differences, if any, were only secondary). The deformations leading to the picture of the stretching of interlamellar amorphous material were carried out on samples with fibre symmetry, and what may be more important, at room temperature. To resolve the differences we shall now take the double texture samples and extend the earlier work down to room temperature.

In addition, a new sample type possessing single texture only will also be introduced in these experiments. As reported previously [7] when low density polyethylene is rolled in only one direction, single textures, such as either the left or the right hand side of fig. 3, are obtained. Each of these textures forms one of the two surface layers of the rolled sheet (in fact, the textures along the two sheet surfaces are in mirror relation just as the left and right sides of fig. 3). In suitable samples these layers can be up to 0.5 mm thick. They can be detached and a sample with true single texture obtained [7]. As they are even simpler than the previously studied double textures their potential for the present experimentation is self evident. These textures are now being intensively studied by Point and

co-workers [16]. A few experiments on the deformation of such single texture material have also been carried out by us and are included in this paper.

Finally, a few isolated earlier experiments on the swelling of double texture samples have shown that the lamellar periodicity can be increased in a characteristic manner by swelling which, at least in one instance, was in quantitative agreement with changes in the long period [5]. These experiments have now been resumed.

## 2. Experimental Techniques

### 2.1. Specimen Preparation

The starting material was low density polyethylene, ICI Alkathene, in pellet form. Sheets of different thicknesses were prepared in a heated press so as to suit the different experimental requirements.

To obtain the double texture samples, sheets were drawn approximately 4x in a tensometer and were then rolled along the draw direction to a thickness reduction of about 0.7x and subsequently heat annealed at the required temperatures.

Single texture specimens were prepared by rolling strips of random sheet, initially 5 mm thick, in one direction only, to a reduced thickness of about 1.4 mm. The single textures required formed along the top and bottom surfaces of the sheet. For further work these surface layers were needed in isolation and were detached by means of a sledge microtome. For this, the sheets had to be clamped without obstructing the sheet plane. To achieve this the sheets had to be glued to a metal surface which provided support and permitted clamping. Glueing of polyethylene to metal, however, is not straightforward: it could nevertheless be achieved after subjecting the surface to low pressure helium ionised in a R.F. field. (This preparation method is due to P. J. Pope, who also assisted with the preparation of the samples used in the present work).

All samples were heat treated at the required temperatures in silicone oil for times of several minutes.

### 2.2. Methods of Straining and Heating

The specimens were stretched or compressed in appropriate frames which fitted into a heater. The whole assembly could be mounted on the specimen holder of the X-ray cameras to be used, and was designed so as to allow the recording of the X-ray diffraction pattern while the sample

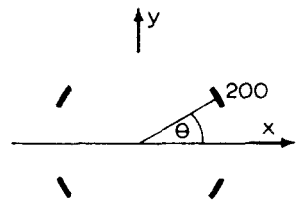


*Figure 4* Sketch defining $\theta$ as determined from a wide angle X-ray pattern taken with the beam along z.

was kept strained at the required temperature (see [17]). The strain was measured by following the separation between ink marks by means of a telescope. The load could be recorded by a modification of the frame illustrated in [18]. The temperature of the sample could be controlled to within $\pm 0.5°C$.

### 2.3. X-ray Diffraction

Both wide and low angle reflections were recorded, the latter with a point focusing Franks low angle X-ray camera. The photographs were taken with the beam perpendicular to y, in the case of double and single textures parallel to z. Past experience has shown that such photographs are the most informative, and that with the background we now possess, a single such photograph suffices to define the samples for our present purpose [4, 7]. The long spacings were assigned by Bragg's law (the quantities measured are defined in fig. 5 – see below). In this we are following existing practice applied to cases where the reflections are unusually sharp by the standards of this subject. The simplications and possible inadequacies inherent in this assignment have been pointed

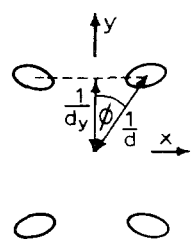


*Figure 5* Sketch showing how the quantities $\phi$, d and $d_y$ are defined in a low angle X-ray pattern taken with the beam along z. $1/d$ and $1/d_y$ are in reciprocal units. The reflections are drawn as hollow lobes where the central portion of maximum intensity is taken to define d. The shape and orientation of the lobes are not referred to in the present paper: this has been done previously in [5].

out repeatedly before (e.g. [4]). The uncertainties involved, however, all relate to the actual numerical value of the size of the structure unit defined by the electron density fluctuation which gives rise to the diffraction peak. The results which follow will only be concerned with changes in the size of these units, hence with differences in spacings; the numerical value of the spacings themselves will be of no consequence. Departures from Bragg's law will only have a second order effect on the differences which we feel we are justified to ignore, particularly as the exact form of such departures, in fact the need for considering such, is problematic.

### 2.4. Measurements

The following quantities were determined from the X-ray diffraction patterns.

Wide angle diffraction: the angle between the 200 maxima and the equator (with the beam along z the equator corresponds to x). In keeping with previous works [4, 7] this angle is denoted by $\theta$ and is to a close approximation equal to the inclination of the 200 plane normal to x, hence to the angle between the chain direction $c$ and y (see fig. 4; for qualifications see [4, 5]).

Low angle diffraction: $\phi$, d and $d_y$ are measured as defined in fig. 5. $\phi$ is the angle between the lamellar normal and y, d is the Bragg spacing corresponding to the lamellar repeat period and $d_y$ its component along y.

To recapitulate, $(\theta + \phi)$ is the chain inclination with respect to the lamellar surface, hence defines the lamellar obliquity (see figs 2 and 3b). This, together with d, was found invariant in the preceding works [5, 6] on externally imposed strains at the elevated temperature of the measurements while both $\theta$ and $\phi$ varied individually so that their sum remained constant. In the past, changes in $d_y$ were not specifically mentioned as they corresponded to the movement of the low angle maxima around their invariant Debye-Scherrer circle which itself was the principal observation [5]. Presently we shall examine our samples as regards possible variations in d and in $d_y$ (to be denoted $\Delta d$ and $\Delta d_y$) – in excess of those due to lamellar rotation alone – and shall attempt to correlate $\Delta d_y$ with $\Delta y$, i.e. with changes in the external sample dimensions along y.

Effects of extension and compression will both be examined. Most of the measurements were carried out at room temperature but a few experiments were conducted at elevated temperatures so as to establish connection with the previous works.

## 3. Results

This section is essentially a catalogue of the principal observations; the evaluation of the results will follow later on in the paper.

### 3.1. Deformation at Room Temperature

#### *3.1.1. Samples with Fibre Symmetry*

The samples were drawn filaments annealed at 85° C. They were extended and compressed along the fibre axis y at room temperature. Wide and low angle X-ray photographs were taken with the beam perpendicular to the fibre axis.

The low angle patterns were essentially meridional streaks with some intensifications at the extremities. The former allowed measurement of $d_y$, while the latter enabled an estimation of d. $\Delta d_y$ and $\Delta d$ determined in this way are shown as a function of $\Delta y$ in fig. 6. On removing the stress compression was found to be almost completely reversible with only 2% permanent deformation. Extension produced 7% permanent deformation. Both samples regained their original dimensions on re-annealing.

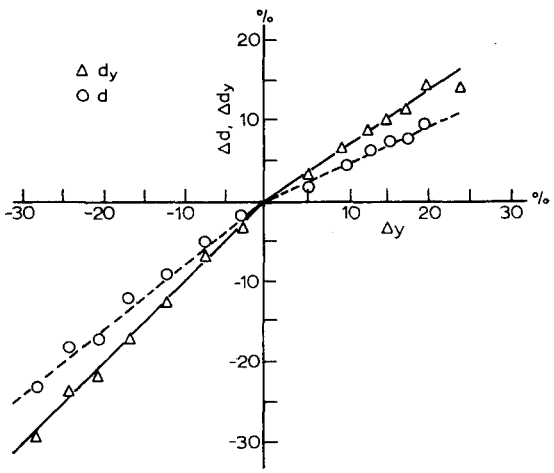


*Figure 6* Spacing changes on extension and compression (at room temperature) of polyethylene fibre texture specimens.

#### *3.1.2. Samples with Double Texture*

This section represents the main body of the experimental work. The choice of sample was guided by the same considerations as in the earlier works on externally induced deformation [6, 8]. Namely, for extension along y and

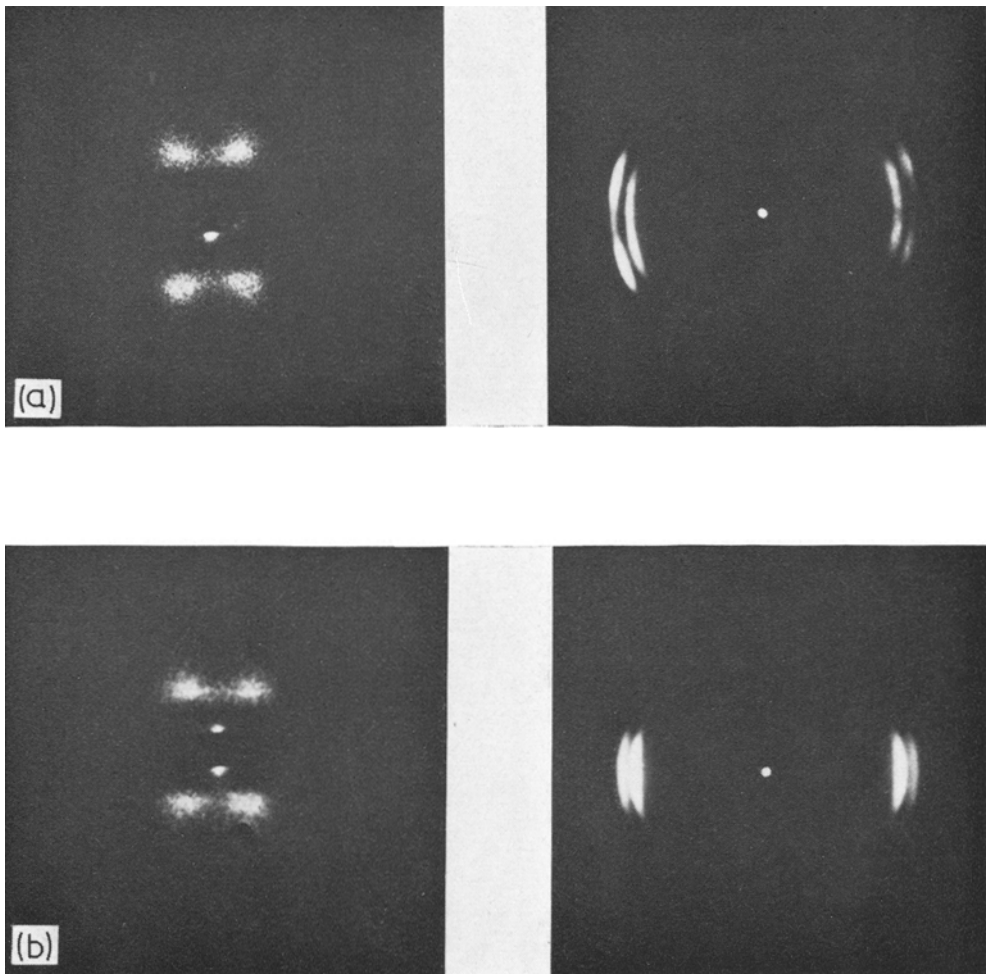


*Figure 7* Effect of extension along y (at room temperature)on low and wide angle X-ray diffraction patterns of double texture specimen annealed at 95°C. (a) $\Delta y = 0\%$ (b) $\Delta y = 20\%$, y is vertical, x is horizontal, beam is along z.

compression along x the samples were comparatively highly annealed so as to possess small $\phi$ and large $\theta$ values, i.e. both chain and lamellar orientations should be far removed from those in the initial unannealed or lightly annealed stages, as the purpose of the stresses applied was to restore this orientation and study the details of this process. Samples annealed at 95 and 99°C were used for these experiments. For the 95°C sample $\theta = 17°$, $\phi = 27°$ and d = 150Å; for the 99°C sample $\theta = 29°$, $\phi = 6°$ and d = 160Å, while both in the initial unstressed state. For compression along y, lightly annealed samples are more favourable so as to give the compression an opportunity to produce large orientation changes. The samples used here were annealed at 83°C. Here $\theta = 13°$, $\phi = 31°$ and d = 110Å.

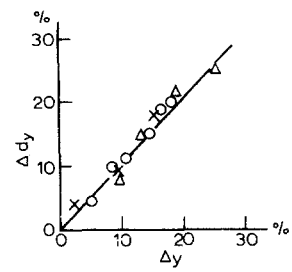


*Figure 8* $\Delta d_y$ (increase) as a function of extension ($\Delta y$) for double texture samples all strained at room temperature.
○ sample annealed at 95°C, extended along y.
△ sample annealed at 99°C extended along y.
× sample annealed at 99°C compressed along x.

*Extension along y*

These experiments were performed on samples

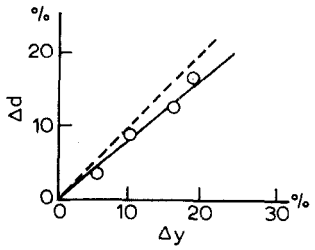


Figure 9

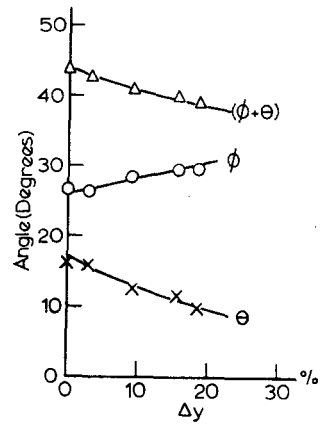


Figure 10

*Figures 9-10* Results of room temperature extension along y of a double texture sample annealed at 95°C.
9 $\Delta$d (increase) as a function of $\Delta$y. (The interrupted line represents the $\Delta d = \Delta y$ relation).
10 $\theta$, $\phi$ and $(\theta + \phi)$ as functions of $\Delta$y.

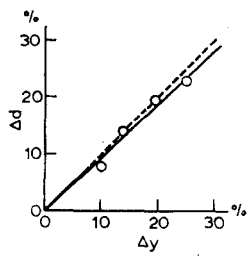


Figure 11

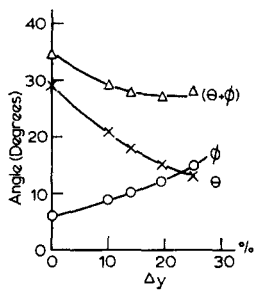


Figure 12

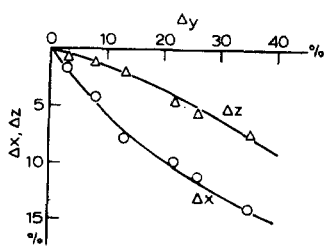


Figure 13

*Figures 11-13* Results of room temperature extension along y of a double texture sample annealed at 99°C.
11 $\Delta$d (increase) as a function of $\Delta$y. (The interrupted line represents the $\Delta d = \Delta y$ relation).
12 $\theta$, $\phi$ and $(\theta + \phi)$ as functions of $\Delta$y.
13 Changes in sample dimensions along x and z ($\Delta$x and $\Delta$z) as functions of $\Delta$y. $\Delta$x and $\Delta$z are negative as they refer to contractions.

annealed at both 95 and 99°C. Typical X-ray patterns are illustrated in fig. 7. Changes in $d_y$ with extension along y followed the same trend for both, and are presented jointly in fig. 8. Changes in d and in the angles $\theta$, $\phi$, together with $(\theta + \phi)$ are shown in figs. 9 and 10 for the 95°C and in figs. 11 and 12 for the 99°C sample. Dimensional changes along the two transverse directions x and z were also measured in the case of the 99°C annealed sample, and are shown by fig. 13. On releasing the stress the permanent deformation was 13% for the 95°C sample with a corresponding change in $d_y$ of 8%, and 5% in the case of the 99°C sample.

*Compression along x*

These experiments were performed only on the sample annealed at 99°C. The $\Delta d_y$ values as a function of $\Delta$y are entered on the graph of fig. 8. The $\Delta$d values are given by fig. 14 and the angles $\theta$, $\phi$, together with $(\theta + \phi)$ are shown by fig. 15. The relation between $\Delta$x and $\Delta$y is given by fig. 16.

*Compression along y*

These experiments were performed on samples annealed at 83°C. A typical X-ray series is illustrated by fig. 17. Fig. 18 shows $\Delta d_y$ as a function of $\Delta$y in several different samples, fig. 19 $\Delta$d as a function of $\Delta d_y$ and fig. 20 the angles $\theta$, $\phi$ and $(\theta + \phi)$ as functions of $\Delta$y. A further graph of $\Delta \cos(\theta + \phi)$ versus $\Delta$d is also included (fig. 21). A striking feature of this compression is the almost complete reversibility, both of the

specimen dimensions and the diffraction patterns. A sample kept overnight under 35% compression showed a permanent deformation of only 2% on stress removal. Recompression of the same sample produced no further permanent deformation.

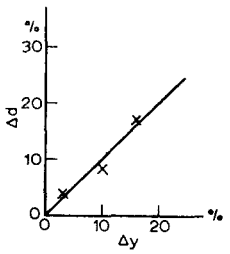


Figure 14

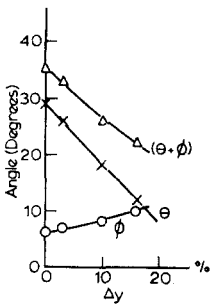


Figure 15

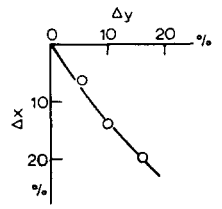


Figure 16

*Figures 14-16* Results of room temperature compression along x of a double texture sample annealed at 99°C (same sample type as in figs. 11-13).
14 $\Delta d$ (increase) as a function of $\Delta y$.
15 $\theta$, $\phi$ and $(\theta + \phi)$ as functions of $\Delta y$.
16 $\Delta y$ as a function of $\Delta x$ ($\Delta x$ is negative as it refers to compression; $\Delta y$ is positive as all through 14-16).

### *3.1.3. Sample with Single Texture*

Systematic examinations were restricted to extensions along y on a specimen which had been annealed at 99°C before cutting. Characteristic X-ray patterns are shown by fig. 22. Comparison with e.g. fig. 7 immediately reveals that only one pair of the split low angle and wide angle maxima are present. It was this kind of pattern by which the existence of single textures was established originally [7]. The effect of the extension on $d_y$ and d is shown by fig. 23, that on $\theta$, $\phi$ and $(\theta + \phi)$ by fig. 24 and that on $\Delta z$ by fig. 25.

Compression along y could only be performed on the intact sheet containing the two single texture zones along its surfaces with the central zone of double texture (see [7]), by taking diffraction photographs of one single texture edge. Bulging of specimens made the measurements of sample size difficult. Two compression measurements at $\Delta y$ of 6% and 12.3% showed changes of 5.5% and 12% respectively in $d_y$. Thus at least it can be said that the single texture deforms in a similar manner to double texture under compression.

## 3.2. Deformation at Elevated Temperature

### *3.2.1. Double Texture*

*Compression along y*

Full series of experiments were carried out only in this deformation mode. The samples used were annealed at 83°C. The compression was carried out at three temperatures: 50, 75 and 83°C, and X-ray photographs taken at the elevated temperature. Fig. 26 shows both $\Delta d_y$ and $\Delta d$ as a function of $\Delta y$. The angles where available are listed in table I. In another experimental series the same type of sample was compressed to $\Delta y = 17\%$ at room temperature and then heated to 75, 80 and 83°C while under pressure. The corresponding $d_y$ values are given in table II.

TABLE I High temperature compression of sample annealed at 83°C

| | | |
|---|---|---|
| 50°C | $\Delta y = 23\%$ | $\theta$ 18° → 31° |
| | $\Delta d_y = 20\%$ | $\phi$ 27° → 16° |
| | $\Delta d = 15\%$ | $\theta + \phi$ 45° → 47° |
| 75°C | $\Delta y = 27\%$ | $\theta$ 19° → 38° |
| | $\Delta d_y = 28\%$ | $\phi$ 27° → 6° |
| | $\Delta d = 19\%$ | $\theta + \phi$ 46° → 44° |

TABLE II Measurements on sample annealed at 83°C compressed at room temperature and heated under compression

| | |
|---|---|
| Room temperature | $\Delta y = 17\%$ |
| | $\Delta d_y = 19\%$ |
| 75°C | $\Delta d_y = 19\%$ |
| 80°C | $\Delta d_y = 16\%$ |
| 83°C | $\Delta d_y = 7\%$ |

*Extension along y*

Only two measurements were made, mainly to

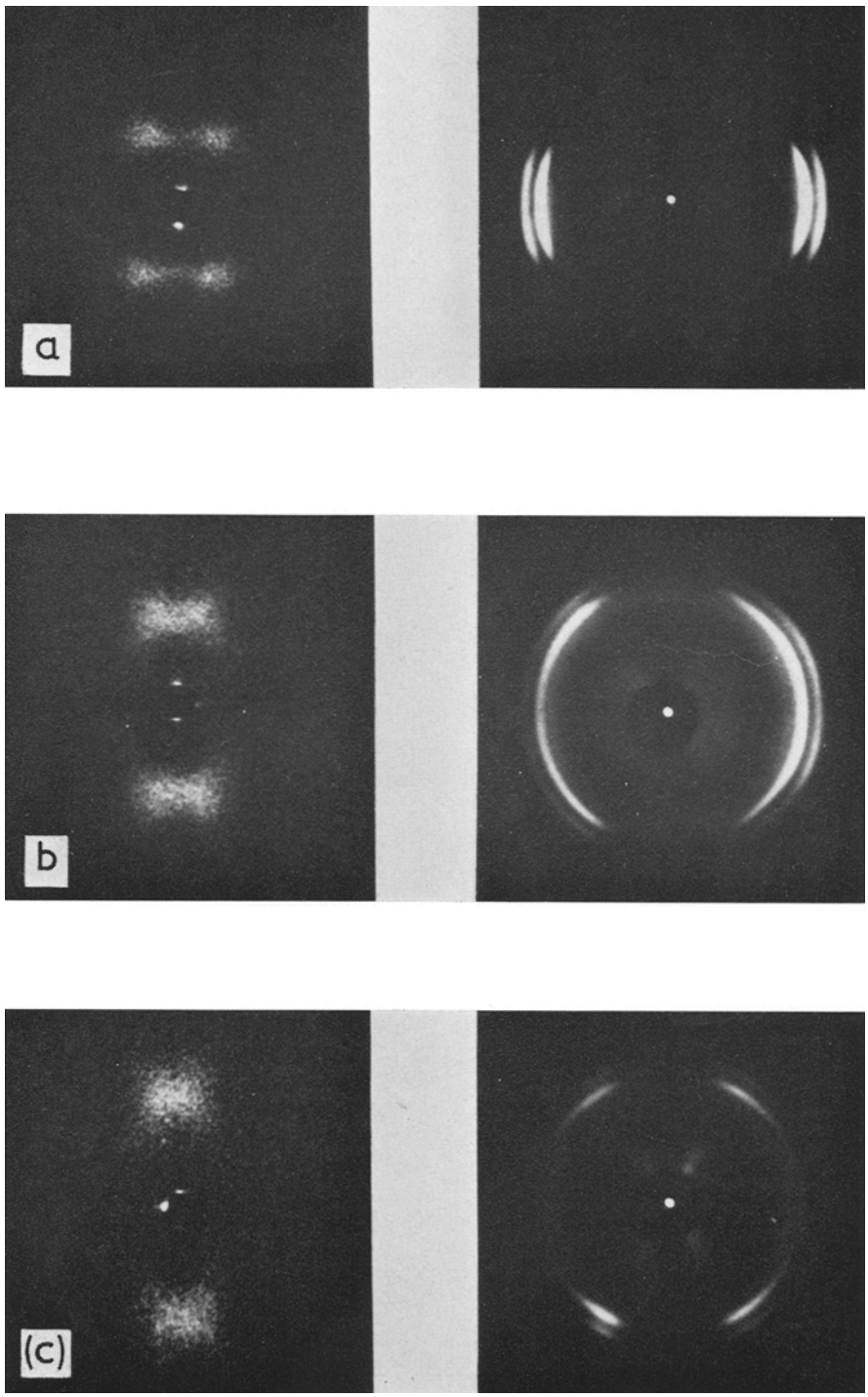


*Figure 17* Effect of compression along y at room temperature on the low and wide angle X-ray diffraction patterns of double texture specimens annealed at 83°C. (a) $\Delta y = 0\%$ (b) $\Delta y = 18\%$ (c) $\Delta y = 35\%$. y is vertical, x is horizontal, the beam is parallel to z.

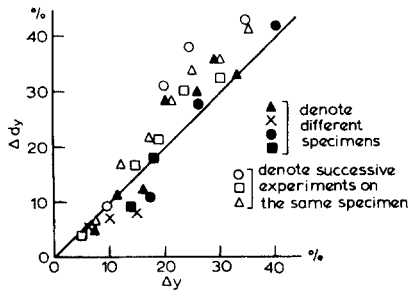


Figure 18

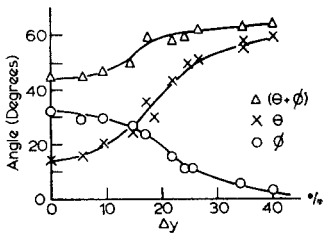


Figure 20

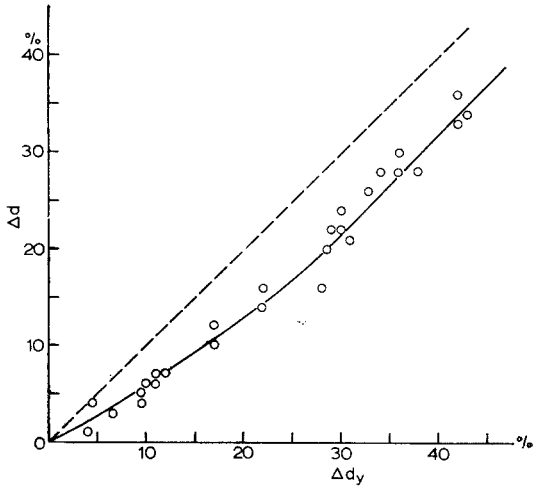


Figure 19

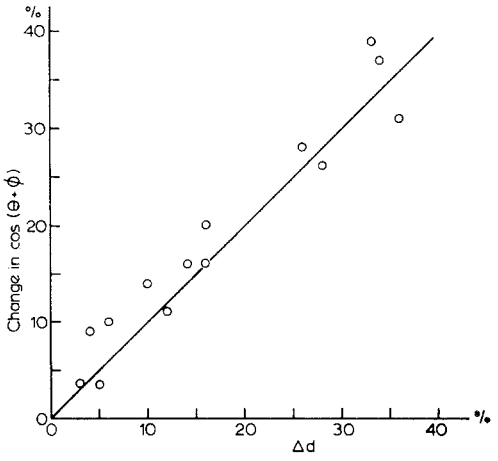


Figure 21

*Figures 18-21* Results of room temperature compression along y of double texture samples annealed at 83° C. $\Delta y$ refers to a reduction of sample dimension.
18 $\Delta d_y$ (decrease) as a function of $\Delta y$.
19 $\Delta d$ (decrease) as a function of $\Delta d_y$ (decrease). (The interrupted line represents the $\Delta d = \Delta d_y$ relation).
20 $\theta$, $\phi$ and $(\theta + \phi)$ as a function of $\Delta y$.
21 Change in cos $(\theta + \phi)$ (decrease) as a function of $\Delta d$.

establish correspondence with earlier works, one at 50°C, the other at 80°C. The samples used were annealed at 95°C. The data on $\Delta d_y$ and $\Delta y$ are contained in table III.

TABLE III High temperature extension of sample annealed at 95°C

| | | |
|---|---|---|
| 50°C | $\Delta y = 15\%$ | $\theta$ 17° → 9° |
| | $\Delta d_y = 13\%$ | $\phi$ 27° → 34° |
| | $\Delta d = 6\%$ | $\theta + \phi$ 44° → 43° |
| 80°C | $\Delta y = 17.5\%$ | $\theta$ 19° → 11.5° |
| | $\Delta d_y = 16\%$ | $\phi$ 26° → 34° |
| | $\Delta d = 5\%$ | $\theta + \phi$ 45° → 45.5° |

### 3.2.2. Single Texture

This part of the work is only fragmentary. Here we report merely that on stretching at 100°C of a specimen originally annealed at 100°C $\Delta d_y$ values of 15 and 26% were recorded for extensions of 15 and 24% respectively.

In the course of such high temperature experiments on single texture samples significant reversible changes in the spacing, d, with temperature were observed: a change from 104 to 153Å. The corresponding diffraction patterns are shown by fig. 27.

### 3.2.3. Load-extension Measurements

A few load-extension measurements were also carried out over the range of temperature and extensions covered by the rest of the work on two double texture samples annealed at 95 and 85°C. No creep was observed during the time of each experiment. Removal of the load at around

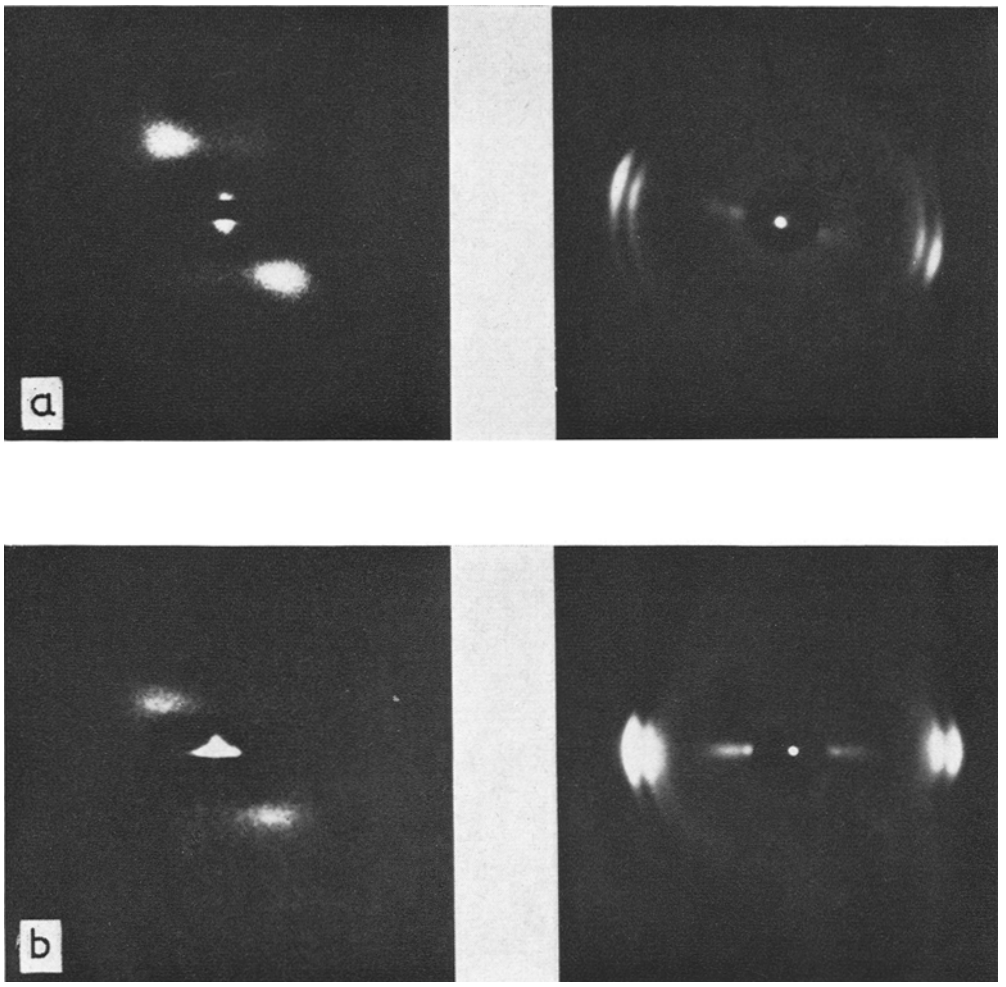


*Figure 22* Effect of room temperature extension along y on low and wide angle X-ray diffraction patterns of single texture specimen annealed at 99° C. (a) $\Delta y = 0\%$ (b) $\Delta y = 21\%$. y is vertical, x is horizontal, the beam is along z.

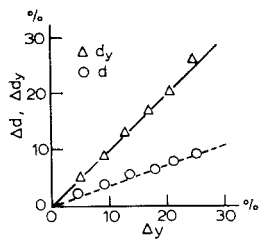


Figure 23

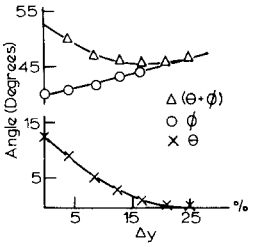


Figure 24

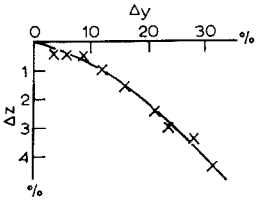


Figure 25

*Figures 23-25* Results of room temperature extension along y of single texture specimen annealed at 99° C.
23 $\Delta d_y$ (increase) and $\Delta d$ (increase) as functions of $\Delta y$.
24 $\theta$, $\phi$ and $(\theta + \phi)$ as functions of $\Delta y$.
25 Change in sample dimension z, ($\Delta z$) as a function of $\Delta z$. $\Delta z$ refers to contraction.

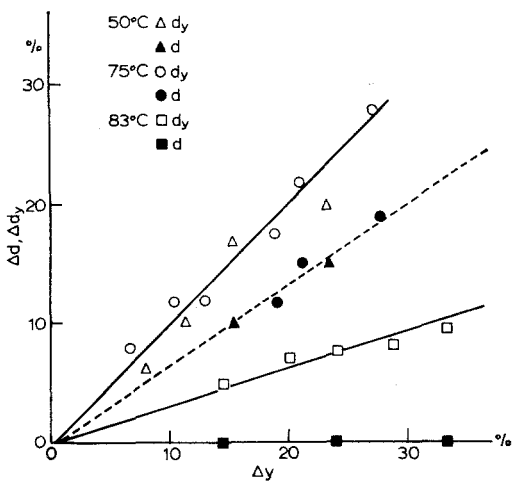


*Figure 26* The effect of compression along y at various elevated temperatures on $\Delta d_y$ and $\Delta d$ (decrease in both cases) in the case of double texture samples annealed at 83° C. $\Delta y$ refers to reduction in specimen dimensions.

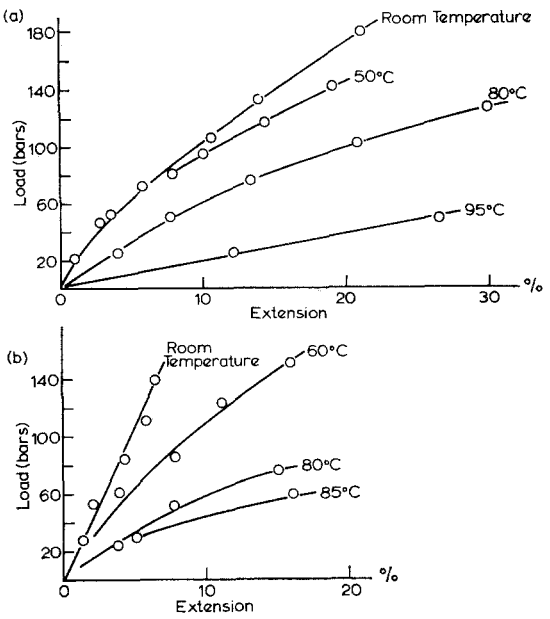


*Figure 28* Load-extension curves of double texture samples at various temperatures.
(a) Specimen annealed at 95° C.
(b) Specimen annealed at 85° C.

20% extension usually left about 5% residual elongation except when specimens were stretched at their annealing temperature, in which case they contracted to their original lengths. The results are shown in figs. 28a and b.

### 3.3. Swelling Experiments

#### *3.3.1. Samples with Double Texture*

A series of samples annealed at temperatures between 75 and 115°C were swollen by immersion in xylene, at room temperature, for several hours. Sample dimensions were measured and low and wide angle X-ray photographs recorded for each specimen before swelling, while swollen and after drying. The changes were almost completely reversible; permanent dimensional changes if observed were less than 1%. Dimensional changes along z were negligible, less than 1%, in agreement with previous findings [1, 5] but changes along other directions were sizeable, $\Delta y$ being larger than $\Delta x$. There were also

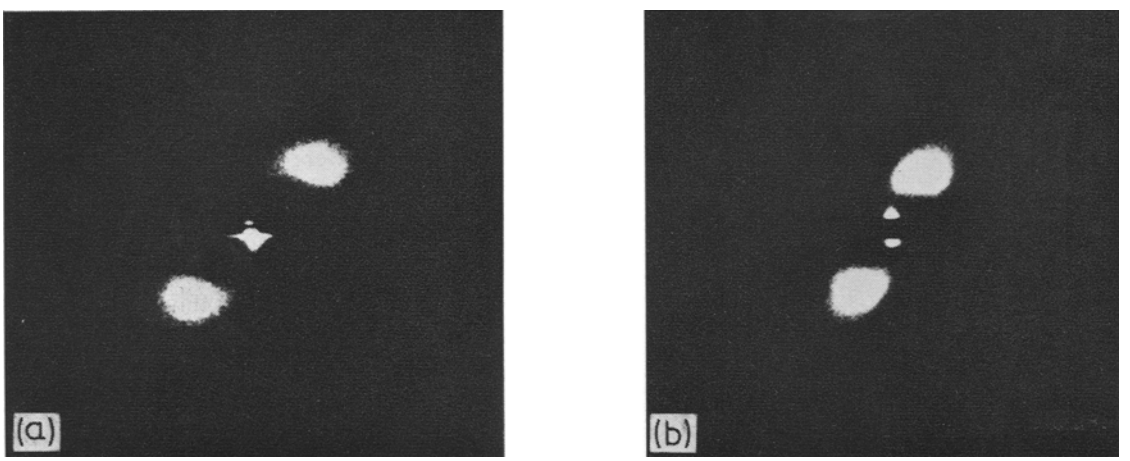


*Figure 27* Low angle X-ray diffraction patterns of single texture specimens annealed at 95° C showing large reversible change in spacing. (a) at room temperature (b) at 95° C. (The sharp cut-off of the reflection at small angles is not due to an obstruction, it is a genuine feature of the pattern).

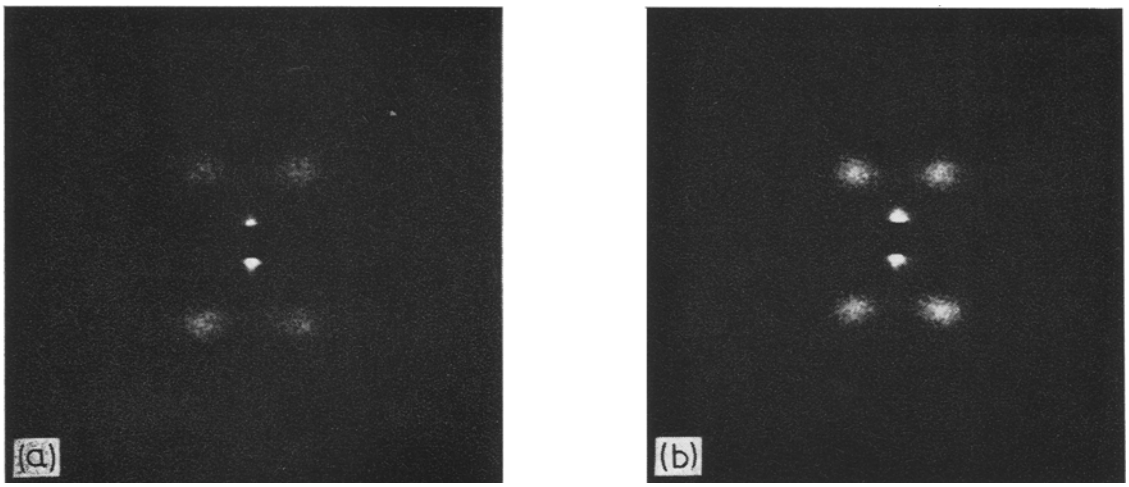


*Figure 29* Effect of room temperature swelling on the low-angle X-ray diffraction pattern of double texture sample annealed at 90°C. (a) Dry (b) Swollen.

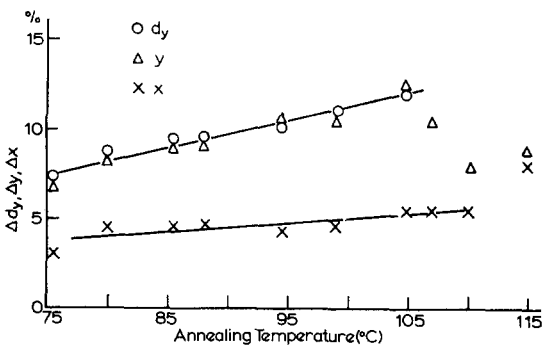


*Figure 30* Increases in spacing $d_y$ ($\Delta d_y$) and increase in sample dimensions y and x ($\Delta y$ and $\Delta x$) induced by the swelling of double texture specimens in xylene at room temperature as functions of the temperature at which the specimens had been annealed prior to swelling.

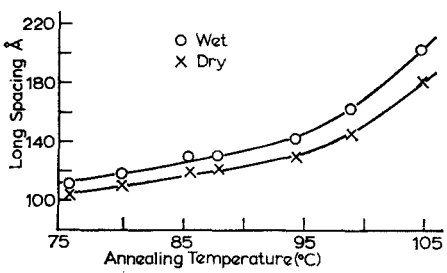


*Figure 31* Long spacing (d) of the same specimens as in fig. 30, with and without swelling agent as functions of the temperature of preceding heat annealing.

reversible changes in the low angle X-ray patterns. Fig. 29 shows an example.

$\Delta y$, $\Delta x$ and $\Delta d_y$ as functions of annealing temperature are displayed in fig. 30.

Changes in the arcing of the wide angle reflections could not be ascertained with any certainty. If there is a change in $\theta$ this must be small. Changes in $\phi$, however, could be detected in the low angle patterns. These amounted to 1 to 2°. It is instructive to express this rotation in terms of $\Delta d_x$ (component of the spacing change along x). This $\Delta d_x$ was readily measurable only in the case of well defined four point patterns where it was 4 to 5%. The actual long spacings for the different samples are recorded in fig. 31.

### *3.3.2. Samples with Single Texture*

A single texture sample annealed at 90°C was swollen at room temperature. Reversible dimensional changes were observed as follows: $\Delta y = 11\%$, $\Delta x = 8\%$, $\Delta z = 1\%$. There were also changes in the low angle X-ray patterns namely: $\Delta d_y = 12\%$; $\Delta d_x = 10\%$ and $\Delta d = 11\%$. We see again a close correspondence between $\Delta y$ and $\Delta d_y$ as throughout most of the work, and also similar even if not as close a correspondence between $\Delta d_x$ and $\Delta x$. The results imply that changes in $\phi$ can only be small if any.

## 4. Analysis of Results

### 4.1. General

Most of the new information in this work is

centred around the relation between changes in $d_y$ as a function of $\Delta y$. In all cases there is a linear relation between $\Delta d_y$ and $\Delta y$ and in the majority of cases $\Delta d_y = \Delta y$.

At first we shall ascertain how the present results tie up with earlier work where the experimental conditions overlap. We see from fig. 6 that in the case of samples with fibre symmetry $\Delta d_y = \Delta y$ for compression but $\Delta d_y < \Delta y$ for tension. This seems to agree with results by Ishikawa *et al* [15]*. Now consider the double texture sample compressed along y at 83°C (fig. 26). We see that $\Delta d_y$ is about a third of $\Delta y$ and $\Delta d$ is zero. As $(\theta + \phi)$ is invariant, all the observed variation in $d_y$ is due to rotation of otherwise unaltered lamellae. This agrees completely with the previous findings of Cowking *et al* [6, 9]. Accordingly, the two apparently conflicting sets of observations we set out to examine have been re-established. (It is to be noted that our X-ray diffraction patterns were taken at the elevated temperature while those in [8] after the sample has been cooled to room temperature subsequent to the deformation. It is apparent that these differences have not affected the results). We shall now proceed to establish a link between these extremes by analysing the origin of these differences in terms of polymer texture, and shall attempt to establish a more general picture of deformation which embraces all observations.

The most conspicuous feature in the majority of our experiments on double and single textures at all but the highest temperatures, is the equality of $\Delta d_y$ and $\Delta y$. This means that in those cases where this relation holds there exists a submicroscopic structure element whose dimensions along the direction of the original draw (y) change in a manner identical to the dimensions of the macroscopic sample along the same direction. Conversely, this means that the macroscopic changes in y can be quantitatively accounted for by the corresponding dimensional changes of submicroscopic texture units. This of course has the important implication, already realised by Slutsker *et al* [14], that for the present deformation studies, the whole sample can be represented as a periodic sequence of such units, and no other structural concept is required. Departures from this behaviour were observed, but even here the linear relation between $\Delta d_y$ and $\Delta y$ is retained with $\Delta y > \Delta d_y$ which means that the changes of the structure period and those of the macroscopic sample dimension remain simply related so that the latter is systematically larger, proportionally by the same amount. This is the case in the extension portion of fig. 6 and in the 83°C curve of fig. 26. (The latter ties up with our earlier works [6] where the quantity $d_y$ was not introduced explicitly as such. Nevertheless, the quantity $\cos\phi/\cos\phi_0$ used there has the same meaning and its linear relation to $\Delta y$ has been amply illustrated.)

We now proceed to re-examine the structural basis of the periodicity $d_y$ and its variations. It is reasonably well established that we have crystal lamellae stacked in a periodic array along y, where the lamellar interfaces are oblique to the chains within the crystal (fig. 2). It is assumed that the stack is broad enough to produce Bragg reflections at an azimuth corresponding to the lamellar normals. We have no direct information on how these stacks are mutually related. Nevertheless the equality of $\Delta d_y$ and $\Delta y$, where this is observed, implies that each stack is contributing equally to the total strain.

According to the above model $d_y$ would represent the periodicity along y within the stack. $d_y$ is related to d by $d_y = d/\cos\phi$, hence will be determined both by the orientation of the lamella defined by $\phi$ and by the Bragg periodicity d. d itself will depend on the length of the straight chain traverse $l$ (which we identify with the fold stems in our chain folded model of lamellae) when allowing for the inclination $(\theta + \phi)$ of these straight chains with respect to the lamellar normals, hence on $l \cos(\theta + \phi)$, and on the thickness of the layer which produces the electron density fluctuation responsible for the low angle X-ray diffraction patterns ($d_a$ in fig. 2). The latter would contain the surface of the crystal, including folds, amorphous layer (as far as the two are different) and interlamellar gap, or in general the discontinuity involved when going from one layer to the next. Now in principle all these quantities can be affected by the applied stress and will all contribute to the $\Delta d_y$ value measured. The purpose of the discussion to follow will be to identify these effects separately.

*Our fig. 6 is virtually identical to fig. 11 of [15]. However, Ishikawa *et al* refer to the ordinate as "long spacing". Their low angle X-ray diagrams, also illustrated, have a four point character. We infer from the correspondence, between our works that the "long spacing" in [15] refers to our $d_y$ and not our d, although explicit statement to this effect is lacking in that paper.

## 4.2. Method

### *4.2.1. Identification of Lamellar Rotation*

This is done directly by measuring changes in $\phi$ from the azimuthal position of the low angle X-ray maxima. Its contribution to $\Delta d_y$ then follows: it corresponds to that portion of $\Delta d_y$ which is due to movement of the maxima along its Debye-Scherrer circle. In this way the effect of $\phi$ on $d_y$ is separated from that of d.

### *4.2.2. Identification and Analysis of Spacing Changes*

Determination of $\Delta d$ is readily achieved. But beyond this we wish to isolate changes in the crystal core from those in the interfacial layer $d_a$. For this we assume that $l$ is not affected by the deformation (i.e. the straight stems do not change their length in the chain folded structure). With $l$ constant, changes in $(\theta + \phi)$ will give the contribution of changes in the lamellar obliquity to $\Delta d$ (hence to $\Delta d_y$). The portion of $\Delta d$ which is left unaccounted for will then correspond to $\Delta d_a$. An uncertainty arises at this stage as regards the value of $l$. We can take two extremes: (*i*) the straight chains traverse the full layer thickness d at the appropriate inclination $(\theta + \phi)$; (*ii*) they traverse only that portion of the total period d which is appropriate for the degree of crystallinity. Case (*i*) assumes no amorphous layer and no gap at the interface, or, if there is an amorphous layer, that the chain orientation across it is preserved. Case (*ii*) assigns the full amorphous content to the interface and denies any continuity of chain orientation across the boundary. A distinction between (*i*) and (*ii*) leads to the difficult problem of the nature of the crystal interface which is not fully resolved in the case of single crystals, hence even less clear in our more complicated system of an oriented bulk sample of a branched polymer. We can safely say, however, that the true situation will lie between the extremes (*i*) and (*ii*) and the analysis will be presented accordingly.

The isolation of $\Delta d_a$ is subject to the same uncertainties as $l$, hence the results will be expressed again between the limits set by assumptions (*i*) and (*ii*). The structural meaning of $\Delta d_a$ again leads back to the problem of the fold surface, or in general crystal interface, and layer packing. It is likely to consist of several components such as pulling out of interlocking or adhering folds, stretching of tie molecules, opening of voids, and of corresponding effects in compression. However, as we have no direct information on such processes in our present data, subdivision of $\Delta d_a$ into its constituents will not be pursued.

In what follows, the individual cases will be evaluated one by one along the lines indicated. We believe that each represents a prototype of the particular deformation mode in question. But apart from the intrinsic significance a given sample type and deformation mode may have in itself, the examples should serve to illustrate how the information content is to be extracted from this type of experimental material.

## 4.3. Individual Cases

### *4.3.1. Cases with $\Delta d_y = \Delta y$*

*Sample with fibre symmetry*

$\Delta d_y$ is only equal to $\Delta y$ in compression. It is seen that there is a very significant spacing change $\Delta d$. However, $\Delta d$ is less than $\Delta y$. Consequently, while $\Delta d$ is the most significant contributory factor to $\Delta d_y$, it does not account for it alone. Hence there must be some lamellar rotation as well. This is immediately apparent from the low angle X-ray photographs where the diffuse low angle maxima along the layer line streak are seen to move closer together towards the meridian. No further analysis was carried out on these patterns.

*Double texture; room temperature deformation*

*Sample annealed at 95°C extended along y.*

Lamellar rotation. We see from fig. 9 that there is a very large change in Bragg spacing which accounts for most of the macroscopic extension of the sample along y. There is nevertheless a small amount of lamellar rotation, 6°, for a sample extension of 19% (curve for $\phi$ in fig.10).

Subdivision of $\Delta d$. For this we have to consider the changes in the lamellar obliquity along the lines laid out above. We see from fig. 10 that $(\theta + \phi)$ decreases, which means that the chains become more perpendicular to the lamellar interface, hence will contribute to the spacing increase. The subdivision of $\Delta d$ into factors due to change in lamellar obliquity ($\Delta(l \cos \theta + \phi)$) and to changes in crystal separation ($\Delta d_a$) for the limiting conditions (*i*) and (*ii*) laid out in the previous section is carried out in fig. 32 and is explained in the caption. Thus when taking the largest experimental $\Delta y$ value of 19% we see that out of the total spacing change of 24Å which ensues from this elongation, the change in lamellar obliquity accounts for 14Å and crystal

separation for 10Å in case (*i*). In case (*ii*) $\Delta(l\cos\theta+\phi)$ is 9Å and $\Delta d_a$ 15Å. As these represent the two extremes it can be stated that the effects due to intralamellar slip and interlayer separation are about comparable. In view of the linear relation of $\Delta d$ and $\Delta(l\cos(\theta+\phi))$ with $\Delta y$

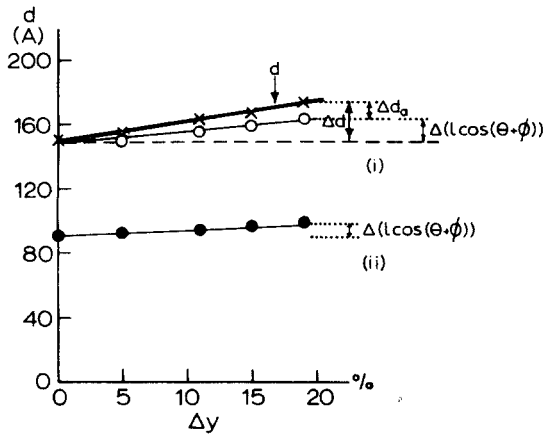


Figure 32

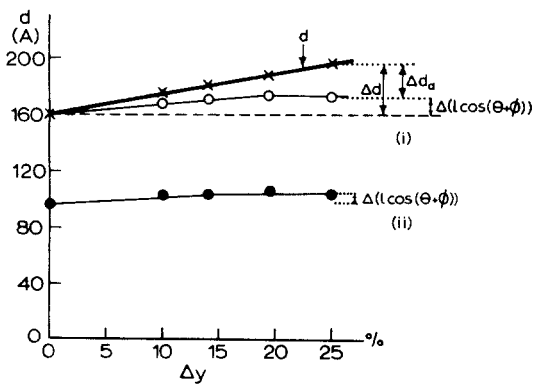


Figure 33

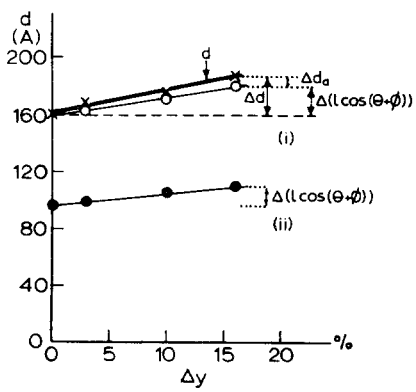


Figure 34

*Figures 32-34* Subdivision of the change in the low angle spacing $\Delta d$ into its constituents $\Delta d_a$ and $\Delta(l\cos(\theta+\phi))$ (changes in lamellar separation and lamellar obliquity respectively – see fig. 2) in case of room temperature deformation of three double texture specimens. The strong line for d represents measured spacing values. The thinner lines connecting the hollow and full circles each represent the changes due to the altered lamellar obliquity on the two assumptions (i) change in chain inclination ($\Delta(\theta+\phi)$) affects equally the whole of the initial lamella (ii) it affects only the region $l\cos(\theta+\phi)$ in fig. 2, the thickness of which is taken to be 60% of the full period d so as to account for the degree of crystallinity (see text). On the right hand side the subdivision is carried out for the largest d value to illustrate the procedure. Here the arrows define $\Delta d$, $\Delta l(\cos(\theta+\phi))$ and $\Delta d_a$ pertaining to this d value. (In case (ii) the appropriate $\Delta d_a$ is obtained by subtraction of the $\Delta(l\cos(\theta+\phi))$ as given under (ii) from $\Delta d$). The same procedure applies to any of the other d values.

32 Double texture sample annealed at 95° C and extended along y (Data from figs. 8-10).

33 Double texture sample annealed at 99° C and extended along y (Data from figs. 8, 11 and 12).

34 Double texture sample annealed at 99° C and compressed along x (Data from figs. 8, 14 and 15).

the same conclusion holds within the whole extension range studied.

*Sample annealed at 99° C extended along y.* Lamellar rotation. Fig. 11 reveals that there is again a considerable change in d, in fact it is numerically closely equal to $\Delta y$. However, this equality does not imply that there is no lamellar rotation. According to fig. 12 (see curve for $\phi$) the lamellae do rotate, 9° for a $\Delta y$ of 25%. Nevertheless in the range of such small $\phi$ values the contribution of this rotation to $\Delta d_y$ is negligible, hence the closeness of $\Delta d$ and $\Delta y$ is practically a corollary of the equality of $\Delta d_y$ and $\Delta y$.

Subdivision of $\Delta d$. There is a decrease of lamellar obliquity of 7° on an extension of 19% as seen from the curve for $(\theta+\phi)$ in fig. 12. It is to be noted that $(\theta+\phi)$ is 35° for zero strain as opposed to 45° for the sample annealed at 95° C. This is in agreement with earlier findings [5] where this was attributed to a transition from a {301} to a {201} lamellar interface on increasing the annealing temperature. The apportioning of the total spacing change to $\Delta(l\cos(\theta+\phi))$ and $\Delta d_a$ is shown in fig. 33 constructed along the same lines as fig. 32. Taking values at $\Delta y = 19\%$ for comparison with the 95° C sample, it is seen that for $\Delta d = 30$Å $\Delta(l\cos(\theta+\phi))$ is 14Å and

$\Delta d_a$ is 16Å for case (*i*). For case (*ii*) $\Delta l \cos(\theta + \phi)$ is 8Å and $\Delta d_a$ is 22Å. As the true value is likely to be between these extremes it appears that increase in lamellar separation has a significantly larger contribution to the total spacing change than the change in lamellar obliquity.

*Sample annealed at 99° C and compressed along x.*
Lamellar rotation. It is seen from fig. 14 that $\Delta d$ is again very close to $\Delta y$ indicating that the effect of lamellar rotation is insignificant. The curve for $\phi$ in fig. 15 indeed reveals only a small change in lamellar orientation which just as in the preceding case of extension along y is within an angular range where its contribution to $d_y$ is insignificant.

Subdivision of $\Delta d$. As seen from the $(\theta + \phi)$ curve in fig. 15 there is now a very significant reduction in lamellar obliquity amounting to around 13° for a $\Delta y$ of 16% which is larger than in any of the preceding cases. As revealed by fig. 34 this now accounts for the larger portion of the changes in $\Delta d$, e.g. for $\Delta d$ of 27Å $\Delta (l \cos(\theta + \phi))$ is 20Å and $\Delta d_a$ is 7Å for case (*i*); the corresponding values for case (*ii*) are 13Å and 14Å in contrast to the behaviour for extension along y. Thus we have a case of a significant amount of intralamellar slip, hence deformation of the crystals, which in this case reduces the lamellar obliquity and contributes to the major portion of the macroscopic strain.

*Single texture; extension along y at room temperature*
Lamellar rotation. Fig. 23 immediately reveals that changes in $\Delta d$ represent only the smaller fraction of the total change in $\Delta d_y$, hence the contribution of lamellar rotation must be significant. Fig. 24 indeed shows that there is lamellar rotation (curve $\phi$) even if its magnitude is comparatively moderate. Nevertheless this rotation is within an angular range (large $\phi$ values) where its contribution to $d_y$ becomes significant, which is the observation.

Subdivision of $\Delta d$. The initial lamellar obliquity $(\theta + \phi)$ is 52° which is higher than in any of the previous cases. Such a high chain inclination in the case of the single texture is in agreement with earlier work [7]. On extension this inclination is first substantially reduced and then it stays constant (curve $(\theta + \phi)$ in fig 24; the slight increase for the point at $\Delta y = 25\%$ would require separate scrutiny). Further analysis of the results along the lines of figs. 32 to 34 revealed that practically the full change in $\Delta d$ was due to a change in $\Delta(l \cos(\theta + \phi))$, i.e. lamellar obliquity. The changes were too small to merit further analysis. Of course the continued linear increase of $\Delta d$ with $\Delta y$ in the range where $(\theta + \phi)$ becomes constant is not compatible with such a correspondence, and therefore a small change in interlamellar separation ($\Delta d_a$) needs invoking for $\Delta y$ of 20 to 25%.

*Compression of double texture at elevated temperatures*
Compressions at 50 and 75° C have led to closely identical results and these will be discussed together.

Lamellar rotation. As apparent from fig. 26 the larger portion of $\Delta d_y$ is due to spacing change $\Delta d$. Lamellar rotation, nevertheless, has a noticeable effect. Values for lamellar rotation ($\phi$) are given in Table I. As seen they are appreciable.

Subdivision of $\Delta d$. As $(\theta + \phi)$ is nearly invariant (table I) there is practically no intralamellar slip and consequently the whole spacing change is constituted largely by $\Delta d_a$. Thus the increase of temperature had the effect of making the separation of the lamellae the only contributory factor to $\Delta d$.

A single experiment extended these compression measurements up to 80° C (table II). $\Delta d_y$ is again very close to $\Delta y$. While further data are not available there is no reason to expect a change in behaviour when going from 75 (table I) to 80° C, in contrast to the large change between 80 and 83° C (see below).

*Extension of double texture samples at elevated temperature*
The behaviour at 50 and 80° C was again closely similar (table III).

Lamellar rotation. Here again $\Delta y$ is close to $\Delta d_y$. As seen, lamellar rotation makes the larger contribution to $d_y$ even though the change in $\phi$ is numerically not very large. Spacing change is small.

Subdivision of $\Delta d$. As $(\theta + \phi)$ is practically constant the small spacing change observed must be essentially due to $\Delta d_a$.

### 4.3.2. Departures from $\Delta d_y = \Delta y$ Relation

*Extension of sample with fibre symmetry at room temperature*
Here $\Delta d_y$ is smaller than $\Delta y$, but only by a factor of 0.7 throughout, i.e. the linear relation between

$\Delta d_y$ and $\Delta y$ is retained. Thus the sample extension exceeds the increase in the submicroscopic periodicity. We see from fig. 6 that the largest portion of $\Delta d_y$ is due to a change in spacing $\Delta d$, nevertheless some lamellar rotation also takes place. These effects were not analysed further.

*Compression of double texture annealed at 83° C along y at room temperature*

In view of the scatter of points in fig. 18, we cannot conclusively say whether the relation $\Delta d_y = \Delta y$ holds or not. What is apparent is that the correlation is not as straightforward as in the earlier cases and that $\Delta d_y$ may even be larger than $\Delta y$. It is visible by inspection of the diffraction patterns (fig. 17) that the compression is associated with large changes in both lamellar orientation and lamellar obliquity (note the large angular separation of the 200 reflection ($\theta$ angle) about the equator in the wide angle pattern associated with the unaltered meridional positions of the low angle maxima in fig. 17c). The scatter notwithstanding, a large amount of intralamellar slip leading to a highly oblique lamellar structure is directly apparent and is expressed by fig. 20. (Note the rise in the $(\theta + \phi)$ curve up to close to 60°).

In view of the large scatter in fig. 18, $\Delta d$ is not expressed in terms of $\Delta y$. Nevertheless when the variations in the X-ray patterns alone are considered (and not its correlation with macroscopic sample dimensions) certain regularities deserve attention. Thus fig. 19 shows that $\Delta d_y$ increases by the same increments as $\Delta d$ at sufficiently high $\Delta d$ values. This is a direct consequence of the effect of lamellar rotation by which the lamellae become progressively more nearly normal to y. When the latter state is reached the change in $\Delta d$ will of course be identical with that in $\Delta d_y$. The approximate equality of $\Delta \cos(\theta + \phi)$ and $\Delta d$ emerging from fig. 21 reveals that within the limits set by the scatter of the points the full spacing change is due to change in chain inclination, i.e. intralamellar slip, and there can only be little if any contribution due to change in lamellar separation.

*Compression of double texture at 83° C*

This is the most conspicuous case of a departure from the equality of $\Delta d_y$ and $\Delta y$ as $\Delta d_y$ is only about a third of the latter throughout the range studied (fig. 26). Here $\Delta d$ is zero, there is no interlamellar shear ($(\theta + \phi)$ remains constant), and the only process which contributes to $\Delta d_y$ is lamellar rotation which we attribute to interlamellar slip. As already stated this has been the principal conclusion of the previous works on this topic. Table II is of special interest. $\Delta d_y$ for 83°C in table II falls on the curve of the 83°C deformation in fig. 26 at the corresponding $\Delta y$ value. Thus a major change in behaviour has taken place between 80 and 83°C. It is to be noted that the $\Delta d_y$ value seems to be uniquely defined by the highest temperature to which the sample, compressed to a particular $\Delta y$ reduction, is raised rather than on the temperature at which the compression is originally applied.

### 4.3.3. Comments on Reversibility

A number of observations were made on the reversibility of strain and on the associated structural changes, some of which have already been listed in the experimental section. The data are not complete enough for a coherent discussion; the following general trends nevertheless deserve noting. Up to 75°C, compression was always more reversible than extension, in fact the reversibility was usually practically complete. At 83°C significant permanent deformation resulted on compression. The residual reversible portion corresponded to the observed reversible change in $d_y$. In contrast a high degree of reversibility was found on extension, as had been reported at such high temperatures previously [5] and observed recently in the load-extension studies. In the high temperature experiments a factor additional to the usual isothermal reversibility arises when the sample is stressed at the elevated temperature, and cooled to room temperature before the stress is removed. Under these conditions some permanent deformation results even under compression. For stressing at 50 and 75°C this is small, e.g. for $\Delta y = 20\%$ at 50°C $\Delta y = 5\%$ at room temperature with an associated $\Delta d_y = 6\%$. (No residual $\Delta d$ is observed, the residual $\Delta d_y$ is solely due to lamellar rotation). When stressed at 83°C and unloaded at room temperature the full $\Delta y$ and $\Delta d_y$ at 83°C is retained.

At this stage the reversibility of the different components of $\Delta d_y$ requires examination. Our data are not complete enough to do this systematically. The following can nevertheless be stated. In the case of complete reversibility on isothermal unloading all components of $\Delta d_y$ revert to their unstressed value. In the non-isothermal experiments there is some reversible change in d with temperature under all circum-

stances (of which fig. 27 is an exceptionally pronounced example – see below). In the case where $d_y$ remains unaltered even when unloaded at room temperature there is a rotation $\Delta\phi$ which compensates for changes in d so that $d_y$ remains constant.

#### *4.3.4. Swelling Experiments*

The principal effect here is the reversible increase of d, an effect which is larger in samples annealed at higher temperatures, both numerically and percentagewise (fig. 30), e.g. for a sample annealed at 75°C the spacing increases by 8Å corresponding to a change of 8%; for a sample annealed at 105°C the corresponding figures are 22Å and 12%. When considering the relation of this spacing increase to the change in sample dimensions we see that $\Delta d_y = \Delta y$. (Beyond 105°C the low angle patterns were too disoriented for the present evaluation. For annealing temperatures of 115°C and beyond, the samples are essentially isotropic in every respect). Measurements such as could be carried out accurately on $\Delta d_x$, suggest that $\Delta d_x$ is equal, or close to, $\Delta x$. As no change in $\theta$ could be recorded and changes in $\phi$ were very small, to a good approximation at least, there is hardly any change in lamellar orientation nor in lamellar obliquity. Accordingly, nearly all the spacing change is due to $\Delta d_a$. This means that the effect of swelling is the separation of the lamellae (or rather their crystalline core) and it is this increased separation which causes the sample to expand and this, in certain cases at least, in quantitative correspondence with the changes in the structure. This quantitative correspondence is always complete for z (i.e. $\Delta z \sim 0$ a fact noted previously [1, 5, 19]) and for y. It is realised for x in cases of a pronounced four point pattern (double texture samples annealed at 75 to 95°C) and is also closely approximated for the only single texture sample which was examined. However in the case of double textures displaying a two point pattern, i.e. when $n_L$//y (samples annealed at 99 to 105°C) no expansion along x would be expected by simple lamellar separation. To account for the $\Delta x$ observed in this case on the basis of a change in $d_x$, lamellar rotation would be required. Within the coalescing meridional spots a change in $\phi$, or for that matter in $d_x$, could not be ascertained. When $n_L$//y (i.e. $\phi \sim 0$) $\Delta d$ is necessarily equal to $\Delta d_y$. It was in this case that the equality of $\Delta d_y$ and $\Delta y$ was noted previously [5].

## 5. Discussion

### 5.1. The Principal Elements of the Deformation

The principal outcome of the present work is the recognition of the structural changes which take place in the deformations considered, and the establishment of the lines along which they can be assessed individually. As seen from the foregoing, it has emerged that in most cases the macroscopic sample deformation can be accounted for by the changes in the submicroscopic periodicity constituted by the lamellar structure. Previous work pointed to the same conclusion [13, 14]. It has, nevertheless, now become apparent that past works have concentrated only on certain aspects of what is now recognised as a broader spectrum of structural processes.

It was stated above that we consider our samples as stacks of parallel lamellae. When strained, each stack deforms by an equal amount corresponding to the macroscopic strain. Thus we can consider a double texture sample as two stacks, a single texture as one stack of lamellae, where the lamellae are coupled in series. The structural processes occurring on deformation can be represented by a series coupling of appropriate elements. Each element of the system will deform as appropriate to its compliance under the same common stress, the different extensions or compressions adding up to the full macroscopic change in sample dimension. In the preceding section we have established these changes individually. We have seen that their proportions differ according to sample type, stress and temperature. In general such differences must be due to the differences in the relative compliances of the components, which are coupled in series within the stack.

We can reduce the system to three such components acting as three visco-elastic elements. When considering the instantaneously reversible portion of the deformation – which as was seen can be the principal portion, or under some circumstances even the sole constituent of the deformation process – each such element will be a spring, a picture we shall use to simplify the qualitative argument to follow. There will be three springs, one for each of the processes involved: the separation of the lamellae ($\Delta d_a$), reversible interlamellar slip ($\Delta\phi$) and reversible intralamellar slip ($\Delta(\theta + \phi)$) respectively (or the appropriate viscoelastic element when the non-reversible and time dependent portion of the processes are considered). The spring constants

for each will be different and of different variabilities. For a given deformation the dominant effect will correspond to the softest spring. We shall now take the three elements in turn.

(1) Lamellar separation. The structural basis of changes in $d_a$ is likely to be the straining of amorphous material between the crystal cores as indeed suggested by Slutsker *et al* [14]. One may expect this to be of a rubbery nature. If this were so it should display the characteristic effect of entropy elasticity, namely that when held stretched under constant load it should contract when the temperature is raised. Some scouting experiments have in fact been performed to this effect on double texture samples in the temperature range of 20 to 80°C. No contraction, but only extension, was observed. It is therefore concluded that energy elasticity is the dominant factor. Such energy elastic effects in stacks of parallel lamellae could be the flexing of superposed, but only partially contiguous lamellae, such as recently postulated in the morphologically related system of "hard elastic fibres" [20-22] (see later). The swelling results, nevertheless, imply that amorphous material does lie between the layers, hence its deformation must contribute to $\Delta d_a$ in addition to any other effect that may occur.

(2) Interlamellar slip. The element representing the process is likely to correspond to tie molecules, including those with large components along the lamellar face, i.e. "amorphous" chains which lie more or less stretched out in that plane. Entangled, interlocking folds from superposed lamellae would also make a contribution. Finally, if the lateral displacement of the lamellae were impeded due to obstruction by neighbouring stacks, this would also represent a resistance, possibly a less well defined one, to the slip and would have to be incorporated in the element.

(3) Intralamellar slip. The element representing this process would have to account for the usual lattice forces involved in the displacement of lattice planes (movement of dislocations). However, these can only encompass recoverable displacements within the yield strain of the lattice proper, which is at smaller strains than observed here. When adjacent lattice planes are displaced by full lattice periods or more (in the case of a polyethylene chain this would correspond to half a period when rotation around the chain axis is permitted) there will be no restoring force from the lattice itself, i.e. the deformation would be plastic. For this reason, at least the largest reversible changes in lamellar obliquity observed at present require non-crystallographic forces in addition to the usual lattice forces, which would arise from the peculiar surfaces of these crystals. Thus if the slip planes cut across fold planes there will be a restoring force due to strained folds. To a lesser extent such forces will be present even when the slip planes are fold planes, as some folds can be expected to cross over from one fold plane to another.

As stated above the spring which is softest under the particular circumstances will dominate in the deformation behaviour. It is from this point of view that different experiments can be surveyed and compared.

### 5.2. The Effect of Temperature

At room temperature the effect of lamellar rotation is small, in fact in the sample annealed at 99°C it is negligible and the strain is primarily due to effects (1) and (3) above. Even if there are differences between different specimens the effects of the two are broadly comparable. On raising the temperature to 50, 75 and 80°C, intralamellar slip is completely suppressed and the effect on $\Delta d$ is due to $\Delta d_a$, with an additional effect due to lamellar rotation. On further temperature increase to 83°C on the other hand, $\Delta d_a$ is suppressed and interlamellar slip becomes dominant.

It is to be noted that the material as a whole becomes more compliant with rise of temperature (fig. 28). Thus in absolute terms the stress required to achieve a given strain drops and the observed variation in deformation behaviour on raising the temperature must be due to relative changes in the compliances of the components within the gradually softening overall structure. With increasing temperature element (3) incorporating lattice forces is expected to become stiffer in relation to elements (1) and (2). This means that intralamellar slip is expected to be suppressed. In other words, stresses required to produce intralamellar slip are not attained at a particular strain, as other structural elements deform first and give rise to the specified change in sample dimension. This agrees with observation. It is the amorphous material which is expected to soften more and thus the increasing contribution of $\Delta d_a$ to the total strain found under compression when going from 20 to 75°C is in accord with expectations.

The above argument, however, cannot be taken further to 83°C and beyond, as

unexpectedly $\Delta d$ becomes zero. Here, interlamellar slip is left as the only component of the deformation. This implies that element (2) has become the most compliant in relation to (1) and (3). This in itself suggests that the forces controlling interlamellar slip are different from those involved in changes of $d_a$. It is to be noted, that for extension, the relation between these two is the reverse at room temperature where $\Delta d_a$ makes the larger contribution. It is to be remembered that at high temperatures there is a large amount of partial melting, which is supposed to correspond to progressive melting from the surface layer downwards [27]. It is evident that this will effect the forces which constrain interlamellar slip. Thus even if the contribution of this effect relative to those due to the other elements cannot be specified *a priori* at least a change in overall behaviour is to be expected at the temperatures where premelting becomes pronounced.

It should be remembered that at 83°C $\Delta d_y \sim 1/3\Delta y$ and thus two thirds of the extension does not correspond to observable changes within the lamellar stack. Nevertheless, the linear relation between $\Delta d_y$ and $\Delta y$, and the complete superposability of compression with extension data [6] indicate a simple connection between macroscopic strain and deformation of the internal structure. This also emerges from the present tests, reported in table II. Here a sample compressed at room temperature, where $\Delta y$ and $\Delta d_y$ are closely similar, was heated to 83°C. This led to a sudden reduction of $\Delta d_y$ to its value in fig. 26 at the appropriate $\Delta y$, which means that the residual portion of the macroscopic strain must be contained by the same unspecified structure element which has to be invoked when the pressure was applied at 83°C, this transfer of strain occurring in a narrow temperature range. The nature of this unspecified structure element has been argued in [6] previously. Here we wish to add a possibility arising from a specific model due to Peterlin and associates (see review [30]). Accordingly the stacks of lamellae themselves could be shifted with respect to each other along their length, this displacement being resisted by tie chains between them (according to the variant by Point *et al* [16] the ties could be stress-induced extended chain crystals). The loosening of such tie molecules (or melting of tie crystals [16]) with increasing temperature would then make this process the dominant element in the deformation (see section 5.7).

### 5.3. Effects of Texture, Annealing Temperature and Type of Stress in the Room Temperature Experiments

Next, the different experiments at room temperature will be compared. Three kinds of comparison will be made: (*a*) between different texture types; (*b*) according to annealing temperature for double texture; (*c*) according to application of stress.

(*a*) Only the relation between single and double textures will be considered. We see that where $\Delta d_y = \Delta y$ applies a larger proportion of $\Delta d_y$ is due to lamellar rotation in the case of single texture compared to other textures. Now the single texture samples have a simpler and a more homogeneous architecture also reflected by their transparency. It is readily conceivable that the lamellae in different stacks will slip more in unison, because all lamellae will slip in the same direction as opposed to two symmetrical slip directions with respect to the stress in the case of double textures. In the latter case, depending on how the two stacks are arranged with respect to each other, the lamellar slip may become obstructed. This would raise the stress enabling other deformation elements such as intralamellar slip or lamellar separation to respond.

(*b*) Samples annealed at higher temperatures deform more by change in $d_a$. This indicates that element (1) becomes more compliant, which in structural terms implies that material between the crystal cores becomes more deformable. Such an inference is in agreement with the whole existing body of knowledge on the effect of annealing in oriented systems. Even in the present work it is borne out by three different lines of observation on the same samples. These are: with increasing temperature of annealing there is a larger contribution of $\Delta d_a$ to $\Delta d$ (the effect just stated), a higher extension of the sample for the same load, i.e. lower modulus (fig. 28), and an increasing change in both $\Delta d_y$ and $\Delta d$ on swelling (figs. 30, 31).

(*c*) In all cases compression produces more intralamellar slip than tension for the same $\Delta y$ and $\Delta d_y$, i.e. element (3) is comparatively more compliant. There is an obvious reason for this when compression and tension, both along y are compared. Intralamellar slip will be most favoured when the maximum resolved shear stress is along *c*, i.e. when $\theta = 45°$. In our experiments $\theta < 45°$ to begin with. As tension will bring the *c*-axis towards y it will reduce $\theta$ further. Compression on the other hand will move *c* away

from y, irrespective of which mechanism applies. Thus, conditions will become increasingly more favourable for intralamellar slip in the course of deformation, which is the effect observed.

Conditions are somewhat more intricate when extension along y and compression along x are compared. It has been observed on the same sample type that compression leads to more intralamellar slip for the same $\Delta y$ and $\Delta d_y$ (figs. 33, 34). We shall now assume that our stack consists of alternating, but otherwise independent regions of an isotropic ($d_a$) and anisotropic region ($l \cos(\theta + \phi)$) as in fig. 2 (of course the condition of independence cannot be strictly true) where the anisotropic unit can only deform along one direction, along that corresponding to the intralamellar slip process (crystallographically $\langle 001 \rangle$ $\{100\}$ slip) while the isotropic component deforms uniformly in all directions normal to the compression x. It is apparent even from qualitative considerations that the deformation of the anisotropic component will contribute by a larger amount to $\Delta y$ on compression than on tension. For our system this will mean that we have more intralamellar slip on compression which is the effect observed.

### 5.4. Dimensional Changes on Deformation and Swelling

As both inter- and intralamellar slip take place by rotation around *b*, which is parallel to z, the z dimension should be unaltered. Indeed, our results show (fig. 13) that on extension along y $\Delta z$ is significantly smaller than $\Delta x$ in agreement with earlier observations [5, 6]. This is in qualitative but not quantitative agreement with expectations, as by the above considerations $\Delta z$ should be zero which it is clearly not. It could be argued that our material contains also an isotropic component which would deform equally along x and z in response to stress along y, which could account for the finite $\Delta z$ observed. This point should be amenable to further tests.

The whole issue is linked with the question of whether the volume is affected in the course of these deformations or not. On the basis of the data in fig. 13 there is a volume increase of 7% for $\Delta y = 35\%$. However, in view of the compounding of errors in the measurements along the individual dimensions, particularly the large error in $\Delta x$ (thickness of films) the reality of this increase would need further ascertaining.

The issue of volume change immediately raises questions as regards the microstructure. Thus, can the isotropic material, presumably in the region of $d_a$, contract laterally when stretched in the course of increased lamellar separation. As it is likely to be in molecular continuity with the crystal core, its dimensional changes along x and z are expected to be constrained. Thus tension would have to lead to the opening of voids between the lamellae. The suggested volume increase and the observed intensity increase in the low angle X-ray reflections are indicative of this happening. In fact, in the recently developed "hard elastic fibres" [20-22] which consist of parallel lamellae (obtained along a different route in more highly crystalline materials than ours) such volume changes can be quite spectacular, leading to low densities, high permeability, very intense low angle reflections etc. and are interpreted as due to lamellar separation in the sense just described. Here most of the macroscopic extension corresponds to an increase in volume. While our present samples are certainly not in the same category as regards the magnitude of the effect, the same factors are likely to play a part in their deformation.

Volume changes can be most directly observed and accounted for in the case of the swelling experiments as here changes in the microstructure ($\Delta d_y$ *and* $\Delta d_x$) can be in close agreement with changes in sample dimension. This is in full agreement with the picture that the increased separation, due to swelling of the interlamellar regions, causes the variations in the macroscopic sample dimensions. (Note that here $\Delta z \sim 0$, also that the low angle X-ray reflections greatly intensify (fig. 29) consistent with solvent penetrating between the lamellae).

However, at annealing temperatures beyond 100°C the structure is as in fig. 3c, hence no contribution to the x dimension would be expected by the above picture. We see from fig. 30 that $\Delta x$ remains, nevertheless, sizeable. Thus either the swollen material within the lamellar stacks bulges out in the x (but not in the z) direction, or there is additional swellable material between the stacks, which could have been created or loosened at the high annealing temperatures (see last section).

On the whole we see that the swelling behaviour usefully supplements the picture arrived at from the deformation experiments. In addition, it provides information on the location of swelling agents in terms of the morphology which can be of interest, e.g. for problems such as plasticisation, dyeing, diffusion (membranes!) etc. It also

links up with studies on the simpler system of sedimented mats of solution grown single crystals [23] where spacing changes analogous to those recorded here were observed, and could be directly interpreted as swelling of the surface layer as crystalline mats are known to have no molecular connection between them.

### 5.5. On the Reversible Changes of the Long Spacing with Temperature

Whether or not the long spacing changes reversibly with temperature has long been a principal issue in arguments concerning the validity, or otherwise, of the equilibrium theories of chain folding. After a number of tests it has been concluded that there is no such reversible change in the case of solution grown single crystals. This, together with a number of other factors, has given overwhelming support to the kinetic approach to chain folded crystallisation (see review [24]).

More recently, however, sizeable reversible long spacing changes have been reported in the case of bulk polyoxymethylene [25]. Following this, smaller reversible spacing changes were noticed in solution grown single crystals of ethyl and methyl branched polyethylene [26] and in double textured oriented branched polyethylene [5]. The latter effect has been repeatedly observed in the course of the present work on double textures. In the meantime Professor Point informed us of an exceptionally large reversibility in the spacing amounting to 30 to 40% with temperature in single texture specimens [16], an effect which we subsequently observed ourselves. The example illustrated in fig. 27, amounting to a reversible spacing increase of 47%, is to our knowledge, the largest observed.

Short of reverting to the equilibrium theories of chain folded crystallisation, it has been proposed that reversible spacing increase with temperature could be due to the increased volume associated with the interfacial melting of the crystals [27, 28]. Even geometric and mechanistic problems apart, it is obvious that such a melting effect cannot yield a spacing change larger than about 15%, particularly as the samples concerned must remain partially crystalline. When applying various correction factors to allow for slit smearing and for the diffuseness of the maxima, the magnitude of the large effect observed in [25] could be reduced so as to bring it within the scope of the premelting explanation [29]. However, in fig. 27 the beam was point collimated and the maxima sharp, and thus corrections as applied to the above mentioned results cannot be invoked. We have no explanation to offer for the effect. Although we have not succeeded in obtaining an effect of this magnitude since, we wish to place this observation on record.

### 5.6. Consequences for Mechanical Properties

The influence of the morphology on the mechanical properties is well recognised. One of the purposes of studying the present simplified textures has been to provide a more concrete structural basis for the interpretation of mechanical measurements than otherwise available. The significant advantages of double texture samples have in fact been profitably exploited in this respect [9, 10], in particular by distinguishing between anisotropy patterns attributable to inter- and intralamellar shear. We see that the present work – in addition to the single textures discovered previously – has greatly widened the scope of this kind of study. In particular, it has drawn attention to further structural processes which set in in various proportions as the temperature is altered and which must all contribute to the overall mechanical behaviour, and thus also to the anisotropy of a given specimen. Similarly, it has drawn attention to the varying proportions of these components in different sample types and to differences in their response to the application of stress which should also be reflected in their mechanical behaviour. Conversely, structural information obtained along the present lines is obviously required for the interpretation of mechanical data in terms of structure.

### 5.7. Some General Comments on the Structure of Oriented Polymers

Some significant structural concepts have emerged from the present results which, even if mentioned in the appropriate parts of the preceding text, deserve restating together. Thus in drawn and/or rolled material, the load bearing elements are stacks of platelets which lie parallel to the direction along which the samples have been *originally* stretched (in heat relaxed samples this need not be the chain direction). On imposition of external stress these parallel stacks all deform by the same amount. According to existing structural concepts the platelets within a given stack are partly chain folded and partly

connected by traversing molecules. Our experiments show that, from a mechanical point of view, a given stack consists of elements of differing compliances coupled in series in an alternating sequence. (The problem of how amorphous and crystalline components are mechanically coupled is basic for mechanical studies, and is not readily resolvable in the general case. The present samples reduce the issue to a specially simple case which should, therefore, be particularly valuable for the study of this problem). It follows that it is the connectedness along the stack direction, and not the lateral extension of the stack, which is of primary significance for mechanical considerations. Thus it should be immaterial how we visualise the subdivision of the sample into individual strands.

The foregoing are all consistent with current pictures of fibre structure and fibre formation as developed particularly by Peterlin (see review [30]). Accordingly, on drawing the lamellae break up into chain folded blocks, a fact which has long been apparent from the beaded structure of filaments pulled out from single crystals. It is such beaded filaments which are supposed to constitute the drawn fibre itself. The circumstances of drawing and heat treatment affect the thickness of the blocks (fold length) which, however, is of no primary concern to us here. They should also affect the structure, hence compliance, of the elements which connect the blocks within a given strand, a factor which has also emerged from the present work when samples annealed at different temperatures were compared. Circumstances of drawing and heat treatment should also affect the lateral register of the blocks, which does not alter the basic mechanical character of the system, but accentuates the low angle reflections, together with the directly observable striated morphology (a line of work not pursued here).

The model of fibre formation referred to [30] also involves interfibrillar material. It is visualised that chains of essentially amorphous character run from one fibril to another and become extended during the *initial* orientation process. At sufficiently high temperatures, when a certain degree of mobility is attained, these stretched chains will contract in a rubbery fashion and cause the sample to shrink. In another version [16] this interfibrillar tie material is visualised as consisting of stress-induced extended chain type crystals where the chains contract on melting of the crystals. Whichever the case, this interfibrillar material would account for the compressive force invoked throughout the preceding works [4-6] to explain the shrinkage observed on annealing and the associated orientation effects attributed to the consecutive occurrence of inter- and intralamellar slip. At the same time the relaxed interfibrillar material would account for the increased compliance at those elevated temperatures. In other words it would produce that portion of $\Delta y$ which is in excess of $\Delta d_y$, i.e. in excess of the effect due to the change in the internal structure of the lamellar stack. This portion of the dimensional change is to be visualised as due to the sliding of the stacks themselves. Owing to the structural connectedness between the stacks, this deformation mode would represent an additional element in the series coupling [6]. It will be the most compliant element at the elevated temperatures in question, but it will stiffen on cooling so that it will cease to contribute to the deformation altogether. It is implicit, therefore, that at these lower temperatures the interfibrillar material cannot be regarded as a rubber any longer. The obvious suggestion is that it crystallises on cooling, in which case it would, however, have to form a kind of crystal which melts before the rest on renewed heating (i.e. between 80 and 83° C in the case of the sample investigated here).

That some material capable of swelling resides between the stacks, in increasing amounts with increasing annealing temperature, has already been suggested. It is tempting to associate such material with interfibrillar links. Nevertheless, the anisotropy of the lateral swelling (no swelling along z) would not follow without further assumptions. Also the reason why such material makes no contribution to $\Delta y$ on the deformation of the dry sample needs consideration. Conversely, from these ideas, deformation experiments in the swollen state suggest themselves.

In conclusion, we see that the interpretation of the present experiments naturally leads to structural concepts which have already been invoked in the course of different lines of work on oriented systems, to which it thus lends added weight. At the same time, the present approach also points to further problems and suggests some obvious further experiments.

## Acknowledgement

One of us (D.P.P.) is indebted to the Science Research Council for financial support during the course of this work.

## References


1. I. L. HAY, T. KAWAI, and A. KELLER, *J. Polymer Sci.* C **16** (1967) 2721.
2. T. SETO and Y. TAJIMA, *Japanese J. Appl. Phys.* **5** (1966) 534.
3. T. SETO, T. HARA, and K. TANAKA, *Japanese J. Appl. Phys.* **7** (1968) 31.
4. I. L. HAY and A. KELLER, *J. Mater. Sci.* **1** (1966) 41.
5. I. L. HAY and A. KELLER, *J. Mater. Sci.* **2** (1967) 538.
6. A. COWKING, J. G. RIDER, I. L. HAY, and A. KELLER, *J. Mater. Sci.* **3** (1968) 646.
7. J. J. POINT, G. A. HOMÉS, D. GEZOVICH, and A. KELLER, *J. Mater. Sci.* **4** (1969) 908.
8. A. COWKING and J. G. RIDER, *J. Mater. Sci.* **4** (1969) 1051.
9. V. B. GUPTA and I. M. WARD, *J. Macromol. Sci.* B **2** (1968) 89.
10. Z. H. STACHURSKI and I. M. WARD, *J. Polymer Sci.* A2 **6** (1968) 1817.
11. C. W. BUNN, *Trans. Faraday Soc.* **35** (1939) 482.
12. A. KELLER, *Ber. Bunsen Ges. Phys. Chem.* **74** (1970) 812.
13. D. R. BERESFORD and H. BEVAN, *Polymer* **5** (1964) 247.
14. A. I. SLUTSKER, T. P. SANPHIROVA, A. A. YASTREBINSKII, and V. C. KUKSENKO, *J. Polymer Sci.* C **16** (1967) 4093.
15. K. ISHIKAWA, K. MIYASAKA, K. MAEDA, and M. J. YAMADA, *J. Polymer Sci.* A2 **7** (1969) 1259.
16. J. J. POINT, M. DOSIÈRE, and A. GOFFIN, Lecture delivered at International Conference on Low Angle X-ray Scattering, Graz, 1970, and private communication.
17. M. J. HILL and A. KELLER, *J. Macromol. Sci.* B **3** (1969) 153.
18. M. J. HILL and A. KELLER, *J. Macromol. Sci.* B, in the press.
19. J. J. POINT, *Mem. Publ. Soc. Sci. Hainaut* **71** (1958) 65.
20. E. S. CLARK, Lecture presented at Gordon Conference on Polymers, New London 1970, and private communication.
21. R. G. QUYNN, H. BRODY, S. E. SOBERING, I. K. PARK, R. L. FOLEY, H. D. NOETHER, W. WHITNEY, R. PRITCHARD, M. A. SIEMINSKI, J. D. HUTCHISON, H. L. WAGNER, K. SAKAOKU, R. CORNELIUSSEN, *J. Macromol. Sci.* B **4** (1970) 953.
22. R. G. QUYNN, Lecture presented at Seventh Annual Synthetic Fibres Symposium, Williamsburg, Va. 1970, and private communication.
23. Y. UDAGAWA and A. KELLER, *J. Polymer Sci.* A2, in the press.
24. A. KELLER, *Reports Progr. Phys.* Part 2 **31** (1968) 623.
25. K. O'LEARY and P. H. GEIL, *J. Macromol. Sci.* B **1** (1967) 147.
26. J. V. DAWKINS, P. J. HOLDSWORTH, and A. KELLER, *Makromol. Chem.* **118** (1968) 361.
27. E. W. FISCHER, *Kolloid Z.u.Z. Polymere* **231** (1969) 458.
28. E. W. FISCHER, R. MARTIN, F. G. SCHMIDT, and G. STROBLE, I.U.P.A.C. Symposium on Macromolecular Chemistry, Toronto, 1968, Preprint A6.17.
29. A. F. BURMESTER, Report T.R. No. 163, Division of Macromolecular Science, Case Western Reserve University, Cleveland, 1970.
30. A. PETERLIN, *J. Mater. Sci.* **6** (1971) 490 and private communication.


Received 14 January and accepted 11 April 1971